International Journal of Earth Sciences (2022) 111:949–968
https://doi.org/10.1007/s00531-022-02161-w

ORIGINAL PAPER

The Jurassic meta-ophiolitic rocks of Cape Steno, Andros, Greece: a high-pressure/low-temperature mélange with Pelagonian affinity in the Cycladic Blueschist Unit?

Melina Höhn[1] · Michael Bröcker[1] · Jasper Berndt[1]

Received: 25 August 2021 / Accepted: 17 January 2022 / Published online: 4 February 2022
© The Author(s) 2022

Abstract

This study aims at clarifying the relationship between the Cape Steno mélange, southern Andros, and the main tectonic units of the Attic-Cycladic Crystalline Belt. Jurassic protolith ages and geochemical characteristics indicate a Pelagonian affinity and point to a correlative relationship with the Tsiknias Ophiolite on Tinos Island. However, jadeitites and high-Si phengite in the gneisses clearly indicate a high-pressure metamorphic overprint that is unknown from the Tsiknias outcrop and other occurrences of the Upper Cycladic Unit. A correlation with the Cycladic Blueschist Unit (CBU) is an obvious assumption, but initially seemed difficult to reconcile with the Cretaceous protolith ages of meta-ophiolitic rocks from the CBU and distinct geochemical characteristics of associated jadeitites. The Jurassic ages of the Cape Steno rock suite either document a broader spectrum of source rocks than previously known from the CBU, or the existence of a distinct tectonic unit. We assume that the geological and tectono-metamorphic evolution of the Cape Steno occurrence is similar to that of the Makrotantalon Unit of NW Andros, which represents a Pelagonian subunit in the nappe stack of the CBU, with abundant slices of serpentinites, rare meta-gabbro and a metamorphic history comprising both Cretaceous and Eocene HP/LT episodes.

Keywords Jurassic ophiolite · Serpentinite · Geochemistry · Andros · Cyclades · Greece

Introduction

The Attic-Cycladic Crystalline Belt (ACCB, Fig. 1a) in the central Aegean region comprises three major groups of tectonic units which record different geological and tectono-metamorphic histories. From top-to-bottom, these groups are referred to as the Upper Cycladic Unit, the Cycladic Blueschist Unit and the Basal Unit (e.g. Dürr et al. 1978; Dürr 1986; Papanikolaou 1987; Okrusch and Bröcker 1990; Ring et al. 2010). The Upper Cycladic Unit (UCU) includes a heterogeneous sequence of unmetamorphosed Permian to Mesozoic sediments, ophiolites with mostly unknown protolith ages, greenschist-facies rocks with Cretaceous to Paleogene metamorphic ages, Late Cretaceous granitoids and amphibolite-facies rocks of the same age (e.g. Patzak et al. 1994; Martha et al. 2016). The Cycladic Blueschist Unit (CBU) consists of a pre-Alpine crystalline basement and several tectonic subunits representing a meta-ophiolitic mélange and a metamorphosed volcano-sedimentary passive margin succession (e.g. Okrusch and Bröcker 1990; Forster and Lister 2005; Ring et al. 2010; Phillipon et al. 2012; Flansburg et al. 2019; Glodny and Ring 2021, and references therein). Between ca. 55 Ma and 12 Ma the CBU was affected by eclogite- to epidote blueschist-facies metamorphism and subsequent overprinting at *P–T* conditions corresponding to the lower pressure blueschist-, greenschist- or amphibolite- facies (e.g. Okrusch and Bröcker 1990; Wijbrans et al. 1990; Bröcker et al. 1993, 2013; Tomaschek et al. 2003; Lagos et al. 2007; Ring et al. 2010; Cliff et al. 2017; Peillod et al. 2017; Laurent et al. 2016, 2017; Lamont et al. 2020b; Glodny and Ring 2021, and references therein). On Tinos, Evia and Samos, metamorphic rocks below the CBU were interpreted as para-authochthonous units, which are separated from the structurally higher sequences by thrust faults (Avigad and Garfunkel 1989; Ring et al. 1999, 2001; Shaked et al. 2000).

A poorly understood aspect of the complex structural architecture of the ACCB concerns the importance of

✉ Michael Bröcker
michael.broecker@uni-muenster.de

[1] Institut für Mineralogie, Westfälische Wilhelms-Universität Münster, Corrensstr. 24, 48149 Münster, Germany

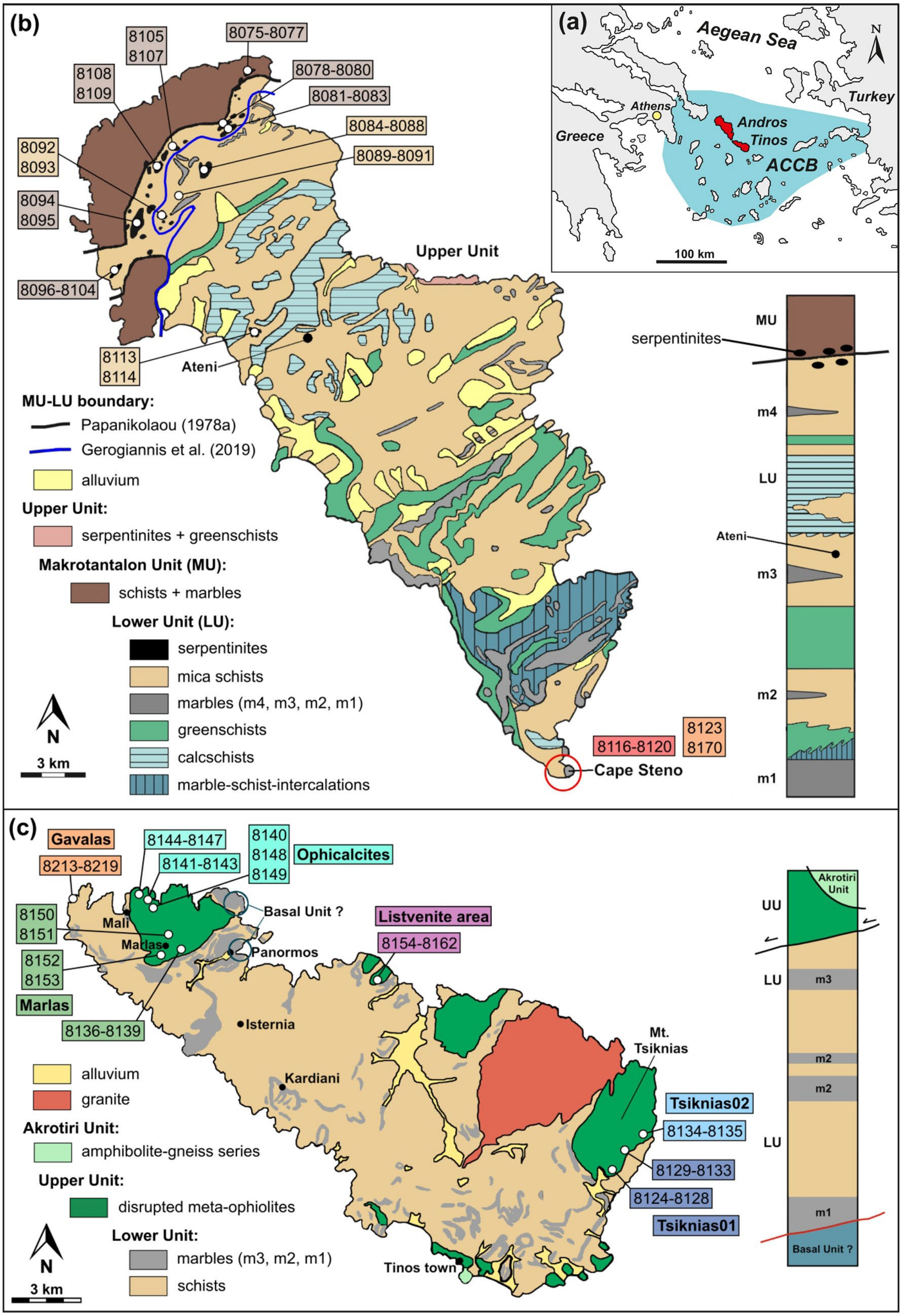
(b)
8105
8107
8075-8077
8108
8109
8078-8080
8081-8083
8092
8093
8084-8088
8089-8091
8094
8095
8096-8104
Upper Unit
8113
8114
Ateni
MU-LU boundary:
Papanikolaou (1978a)
Gerogiannis et al. (2019)
alluvium
Upper Unit:
serpentinites + greenschists
Makrotantalon Unit (MU):
schists + marbles
Lower Unit (LU):
serpentinites
mica schists
marbles (m4, m3, m2, m1)
greenschists
calcschists
marble-schist-intercalations
N
3 km
8116-8120
8123
8170
Cape Steno
MU
serpentinites
m4
LU
Ateni
m3
m2
m1
(a)
Aegean Sea
N
Turkey
Athens
Greece
Andros
Tinos
ACCB
100 km
(c)
Gavalas
8213-8219
8144-8147
8141-8143
8140
8148
8149
Ophicalcites
Basal Unit ?
Mali
8150
8151
Marlas
8152
8153
Panormos
Marlas
Listvenite area
8154-8162
8136-8139
Isternia
Kardiani
Mt.
Tsiknias
Tsiknias02
8134-8135
8129-8133
8124-8128
Tsiknias01
alluvium
granite
Akrotiri Unit:
amphibolite-gneiss series
Upper Unit:
disrupted meta-ophiolites
Lower Unit:
marbles (m3, m2, m1)
schists
N
3 km
Tinos town
Akrotiri Unit
UU
LU
m3
m2
m2
LU
m1
Basal Unit ?

◂**Fig. 1** **a** Geographical overview of the larger study area. *ACCB* = Attic-Cycladic Crystalline Belt. Simplified geological maps and columnar sections of **b** Andros (modified after Papanikolaou 1978a and Gerogiannis et al. 2019) and **c** Tinos (modified after Melidonis 1980) with approximate sample locations

Jurassic meta-ophiolitic rocks that are exposed at the southern promontory of Andros Island (Cape Steno, Fig. 1b; Mukhin 1996; Bröcker and Pidgeon 2007; Bulle et al. 2010). Field observations led to the conclusion that this occurrence was affected by high-pressure/low-temperature (HP/LT) metamorphism and thus can be correlated with the CBU of NW Tinos (e.g. Buzaglo-Yoresh et al. 1995; Bulle et al. 2010). However, such a relationship has not been clearly established yet and it is uncertain whether the block-in-matrix sequence of NW Tinos, located directly across from Cape Steno (Buzaglo-Yoresh et al. 1995; Bulle et al. 2010), represents a lateral equivalent of the Cape Steno occurrence, or was formed at different times and by different processes. Ion microprobe U–Pb zircon dating of Cape Steno meta-gabbros and gneisses yielded Jurassic protolith ages (ca. 174–156 Ma; Bröcker and Pidgeon 2007; Bulle et al. 2010) suggesting a relationship to the ophiolites of the larger Balkan region (e.g. Robertson 2002; Lamont et al. 2020a, and references therein). Jurassic meta-ophiolitic rocks were also described from the Upper Unit of the Tsiknias area on Tinos (Fig. 1c; Lamont et al. 2020a), whereas meta-gabbros in mélanges of the CBU on Tinos, Syros and Samos yielded only Late Cretaceous protolith ages (Keay 1998; Tomaschek et al. 2003; Bulle et al. 2010; Bröcker and Keasling 2006; Bröcker et al. 2014). The relationship of the Cape Steno serpentinite-meta-gabbro-gneiss association to ultramafic rocks exposed in NW Andros is unclear (Fig. 1b; Papanikolaou 1978a, b; Gerogiannis et al. 2019).

This study attempts to clarify the status of the Cape Steno occurrence within the regional context. We combine field observations with new and existing mineralogical, geochemical and geochronological (U–Pb, Rb–Sr) data to unravel litho- or tectonostratigraphic relationships between the Cape Steno occurrence and the meta-ophiolitic rocks of NW Andros and Tinos. An extensive data set for meta-gabbros from both islands is already available (Bulle et al. 2010; Bröcker et al. 2014; Lamont et al. 2020a) but no corresponding information for associated serpentinites. To close this gap, we systematically determined the bulk rock geochemistry of ultramafic rocks from Andros and Tinos and evaluated the mineral chemistry of chromian spinels as indicator of the tectonic environment. The bulk rock composition of serpentinites records the influence of protolith geochemistry, mineral assemblage, fluid-rock interaction as well as later alteration during submarine and subaerial weathering but original REE and trace element abundances are often considered to have been largely preserved (e.g. Deschamps et al. 2013, and references therein; Cooperdock et al. 2018).

The focus of our study is placed on regional aspects. Petrogenetic considerations resulting from this data will be discussed elsewhere. We will show that the originally assumed correlation of the meta-ophiolitic Cape Steno rock suite with the blueschist sequences of NW Tinos is most likely wrong and that a relationship to the Makrotantalon Unit of NW Andros is instead more likely.

Geological background

On Andros, the metamorphic succession can be subdivided into three tectonic units, the Upper Unit, the Makrotantalon Unit and the Lower Unit (Papanikolaou 1978a, b). The Upper Unit (UU), which in the regional context is correlative with the UCU, is poorly preserved (Fig. 1b) and comprises an ultramafic breccia overlain by greenschists and serpentinites that are separated from the structurally lower sequences of the CBU by an extensional detachment (Mehl et al. 2007). Samples from the structurally lower rock sequences, collected close to the tectonic contact, yielded Oligocene Rb–Sr dates (29–25 Ma) of unclear geological significance that either indicate the time of shear zone activity (Huyskens and Bröcker 2014) or incomplete resetting of the isotope system.

The CBU is represented by two subunits, which are described in the regional literature as Makrotantalon Unit and Lower Unit, respectively. The Makrotantalon Unit (MU; up to 600 m thick; Fig. 1b) lies structurally on top of the LU (Papanikolaou 1978a, b; Bröcker and Franz 2006). The MU mainly consists of dolomitic marbles, various types of metabasic and metasedimentary schists and serpentinites (Papanikolaou 1978a, b; Gerogiannis et al. 2019). Fossils in MU marbles yielded Permian ages (Papanikolaou 1978a, b), whereas U–Pb zircon dating of meta-igneous and clastic metasedimentary rocks of the LU indicate Triassic to Early Cretaceous protolith or maximum sedimentation ages (Bröcker and Pidgeon 2007; Bröcker et al. 2016). This old-over-young relationship suggests that the tectonic contact originated as a thrust fault. However, there is no structural evidence for a later reactivation as a low-angle normal fault, as assumed by Huyskens and Bröcker (2014). Instead, Gerogiannis et al. (2019) showed that the original contact was folded during exhumation and transposed by NE-directed thrust-sense shear zones.

Ar–Ar and Rb–Sr geochronological data indicate that the MU records a polymetamorphic history including an Early Cretaceous HP/LT event, a Late Cretaceous greenschist- to amphibolite-facies episode, Eocene blueschist-facies metamorphism and Miocene greenschist-facies retrogression (Bröcker and Franz 2006; Huyskens and Bröcker 2014; Huet et al. 2015; Gerogiannis et al. 2019). The preservation of pre-Eocene blueschists led Huet et al. (2015) to suggest a Pelagonian affinity. Other studies interpreted the MU as an integral part of the CBU because this tectonic slice was also affected by Eocene HP/LT metamorphism (Huyskens and Bröcker 2014; Gerogiannis et al. 2019).

The volcano-sedimentary sequence of the Lower Unit (LU, up to 1200 m thick) comprises clastic metasediments, carbonate-rich schists, calcitic marbles and meta-volcanic rocks (Papanikolaou 1978a, b; Bröcker and Franz 2006). Disrupted bodies of ultramafic, gabbroic and meta-acidic rocks occur at different lithostratigraphic levels and represent either meta-olistostromes, tectonic mélanges, or macro-boudins (Papanikolaou 1978b; Mukhin 1996; Bröcker and Pidgeon 2007; Bulle et al. 2010). The LU was affected by HP/LT metamorphism (450–500 °C, > 10 kbar) in the Eocene at ca. 44–39 Ma (Bröcker and Franz 2006; Huyskens and Bröcker 2014). Strongly overprinted greenschist-facies rocks mostly yielded Miocene dates (ca. 23–21 Ma; Bröcker and Franz 2006).

The Cape Steno mélange at the southern tip of Andros (Fig. 1b) mainly includes non-deformed to variably sheared meta-gabbros, felsic gneisses, meta-basalts, and serpentinites, which are squeezed in between a marble-schist sequence and slivers of schists (Papanikolaou 1978a, b; Buzaglo-Yoresh 1995; Mukhin 1996; Bröcker and Pidgeon 2007; Bulle et al. 2010). Mineral assemblages indicate low- to medium-pressure metamorphic conditions except for a quartz-free jadeitite with a presumed HP/LT mode of formation (Buzaglo-Yoresh 1995). U–Pb zircon dating of meta-gabbros and gneisses yielded Jurassic protolith ages (ca. 174–156 Ma; Bröcker and Pidgeon 2007; Bulle et al. 2010). These rocks were interpreted to represent SSZ-type (supra-subduction zone) ophiolites, linked to the Vardar Ocean or a different coeval oceanic basin (Bröcker and Pidgeon 2007). Fu et al. (2015) questioned a SSZ origin and used oxygen and hafnium isotope data to show that these rocks may be related to partial melting in a metasomatized mantle wedge with significant assimilation of supracrustal material. The marble-schist sequence below the Cape Steno mélange represents the topmost part of the LU on Andros (Papanikolaou 1978a, b; for a contrasting view see Mukhin 1996).

On Tinos (Fig. 1c), the metamorphic succession can be subdivided into at least three tectonic subunits: the Akrotiri Unit, the Upper Unit, and the Lower Unit (Melidonis 1980; Okrusch and Bröcker 1990). The Akrotiri Unit (300–350 m thick) mainly consists of epidote-bearing amphibolites and quartzo-feldspathic gneisses which either represent a tectonic slice of the Upper Unit or a distinct tectonic unit that is unrelated to other subunits on this island (Patzak et al. 1994; Katzir et al. 1996; Lamont et al. 2020a). K–Ar hornblende dating yielded Cretaceous dates (ca. 77–66 Ma; Patzak et al. 1994).

The Upper Unit (UU) comprises lenses and fragments (up to several hundred meters in size) of serpentinites, meta-gabbros, meta-plagiogranites, ophicalcites and listvenites that are embedded in or associated with mostly metabasic phyllites (Melidonis 1980; Katzir et al. 1996; Bröcker and Franz 1998; Zeffren et al. 2005; Lamont et al. 2020a; Mavrogonatos et al. 2021). The UU does not record any evidence of a HP/LT metamorphic event and is considered to belong to the Upper Cycladic Unit (e.g. Katzir et al. 1996; Bröcker and Franz 1998; Zeffren et al. 2005). The meta-ophiolitic rock sequence on Tinos records amphibolite-facies metamorphism followed by a greenschist-facies event (Katzir et al. 1996; Bröcker and Franz 1998; Zeffren et al. 2005). U–Pb zircon dating of a plagiogranitic sill and a meta-gabbro from the Tsiknias area (Fig. 1c) yielded Jurassic protolith ages of ca. 162 Ma and ca. 144 Ma, respectively, and suggests a relationship to the Pelagonian ophiolites of mainland Greece (Lamont et al. 2020a). Amphibolites interpreted to represent the metamorphic sole yielded Cretaceous U–Pb zircon ages between ca. 64 and 113 Ma (Lamont et al. 2020a). Tectonic juxtaposition of the UU onto the LU was achieved by a low-angle normal fault (e.g. Avigad and Garfunkel 1989; Brichau et al. 2007) and probably occurred during a regional greenschist-facies episode at ca. 21 Ma (Bröcker and Franz 1998).

The metamorphic succession of the Lower Unit (LU; ca. 1250–1800 m in thickness) mainly comprises siliciclastic metasediments, marbles as well as mafic and felsic meta-volcanic rocks (Melidonis 1980; Bröcker et al. 1993). Isolated blocks and tectonic slices of meta-gabbros, glaucophanites, eclogites, jadeitites and ultramafic rocks (mostly < 1–10 m, but up to 300 m) occur at various levels within the marble-schist sequence (Bröcker and Enders 1999; Bulle et al. 2010). The matrix is primarily composed of clastic metasediments, while some rock fragments are surrounded by thin serpentinite or chlorite schist (Buzaglo-Yoresh 1995; Bulle et al. 2010). U–Pb zircon dating of meta-igneous blocks yielded Cretaceous ages of ca. 80 Ma (Bulle et al. 2010). The LU has experienced HP/LT metamorphism (> 15–26 kbar, 450–570 °C) at ca. 53–46 Ma (e.g. Bröcker et al. 1993; Parra et al. 2002; Bulle et al. 2010; Lamont et al. 2020b). Remnants of HP/LT rocks are locally preserved, but pervasively retrogressed rocks with greenschist-facies mineral assemblages are more common (e.g. Bröcker et al. 1993; Bulle et al. 2010). This low-grade metamorphic overprint (7–10 kbar, 350–530 °C) took place at ca. 31–21 Ma (e.g. Bröcker et al. 1993, 2004; Bröcker and Franz 1998; Parra et al. 2002).

The lowermost part of the metamorphic sequence is exposed in NW Tinos near Panormos (Fig. 1c). Here, a tectonic contact separates calcite-rich marbles (> 50 m) intercalated with thin bands of quartzites from a discontinuous horizon of phyllites and quartzites (< 2 m thick), which are underlain by dolomite marbles (> 100 m; Avigad and

Garfunkel 1989). Melidonis (1980) and Bröcker and Franz (2005) interpreted the basal sequence as part of the LU, whereas Avigad and Garfunkel (1989) interpreted the dolomites and phyllites as part of a para-autochthonous Basal Unit, as also described from Samos and Evia (Ring et al. 1999, 2001; Shaked et al. 2000).

Sampling and analytical methods

Newly collected samples from Cape Steno represent serpentinites and mica schists from the mélange as well as clastic metasedimentary rocks, calcschists and greenschists from the underlying marble-schist sequence. Ultramafic rocks were also collected from various serpentinite bodies of the MU and LU in NW Andros (Fig. 1b). On Tinos, ultramafic rocks were collected from four major occurrences of the UU (Tsiknias, Marlas, listvenite and ophicalcite areas; Fig. 1c). Furthermore, meta-gabbros, schists and gneisses were taken from outcrops at the NW coast close to Aghios Theodoros (Gavalas area; Fig. 1c). Thin sections of previous studies (Bröcker and Pidgeon 2007; Bulle et al. 2010) were re-examined for indications of HP/LT metamorphism. GPS coordinates are reported in Online Resource 1. Field images are shown in Fig. 2.

The mineral assemblages of most ultramafic rocks consist of serpentine polymorphs (mostly antigorite as confirmed by XRD analysis of representative samples) with minor amounts of chlorite, talc, carbonates, chromian spinel and magnetite. Chlorite is the dominant silicate phase in two samples from NW Andros (8077, 8091) and four serpentinites from Cape Steno (8116, 8117, 8118, 8120). Some samples contain carbonates (calcite, magnesite). Most ultramafic rocks are completely serpentinized. Relic pyroxene and olivine were only found in ultramafic rocks from the Tsiknias area (8129, 8135). Variably altered chromian spinels occur as disseminated grains in the serpentinitic matrix. Magnetite forms rims around chromian spinel, and also occurs in irregular networks and as fine grains.

The Cape Steno mélange includes a lensoid block of jadeitite (Buzaglo-Yoresh 1995). The mineral assemblage of sample 5100 from this occurrence mainly consists of two types of sodic clinopyroxene (colourless jadeite, greenish omphacite; > 85 vol.% pyroxene), plagioclase, epidote and white mica. Omphacite and albite occur as secondary phases. Titanite and apatite are accessory minerals. Sample 5100 was previously U–Pb dated by Bulle et al. (2010) and incorrectly described as gneiss but jadeitite or Jd-Omp granofels are more appropriate rock names. The complex age range of the zircon population led to the interpretation that sample 5100 is of metasedimentary origin but a meta-igneous origin with zircon crystals recording inheritance is more likely.

Samples 8123 and 8170 were collected from the marble-schist sequence below the Cape Steno mélange near Aghios Stephanos (Fig. 1b). Sample 8123 is a calcschist that was selected for Rb–Sr dating. The mineral assemblage consists of calcite, quartz, phengite, epidote, plagioclase and titanite. Sample 8170 is a calcite-rich mica schist that was used for U–Pb zircon dating. The mineral assemblage comprises quartz, calcite, phengite, chlorite and plagioclase. Titanite, rutile, tourmaline and zircon are present as accessory phases.

The meta-gabbros collected near Aghios Theodoros in NW Tinos (Fig. 1c; Gavalas area, samples 8213–8219) have isotropic to well-foliated fabrics and are strongly saussuritized. The mineral assemblages consist of zoisite, epidote/clinozoisite, calcic amphibole, chlorite, white mica and carbonates, in variable modal proportions. Magmatic clinopyroxene is sporadically preserved. The associated siliciclastic schists have a mylonitic fabric and mineral assemblages comprising calcite, plagioclase, quartz, phengite, chlorite, graphite and tourmaline.

Analytical methods (electron microprobe, whole rock geochemistry, U–Pb and Rb–Sr geochronology) are described in Online Resource 2. Analytical data is summarized in Online Resources 4, 5, 6.

Results

Mineral chemistry

Serpentine compositions are dominated by SiO_2 (38.9–45.3 wt%) and MgO (32.9–42.1 wt%). Variable FeO and Al_2O_3 contents range from 0.83 to 10.8 wt% and 0.10 to 3.8 wt%, respectively. The serpentine minerals contain up to 0.30 wt% TiO_2 and 0.59 wt% NiO. Only the Cr_2O_3 concentrations vary among samples from Andros and Tinos. The highest amounts of Cr_2O_3 were detected in samples from NW Andros (up to 3.9 wt%), the lowest in ophicalcites from Tinos (0.11–0.46 wt%). The Cr_2O_3 concentrations in serpentine from Cape Steno and Mt. Tsiknias ultramafic rocks range from 0.10–0.89 wt% and 0.13–0.77 wt%, respectively.

Chlorites in ultramafic rocks from NW Andros contain 26.7–29.9 wt% SiO_2, 21.8–27.2 wt% MgO, and 18.2–21.7 wt% Al_2O_3. They are characterized by variable FeO concentrations (8.2–16.6 wt%) and minor amounts of TiO_2 (0.29–0.34 wt%) and NiO (0.28–0.81 wt%). Cr_2O_3 concentrations are < 0.20 wt%. Cape Steno chlorites have higher SiO_2 (31.3–37.3 wt%) and MgO (28.8–35.4 wt%) contents but lower Al_2O_3 (7.9–17.4 wt%) and FeO (3.0–11.3 wt%) concentrations. NiO values range from 0.22 to 0.35 wt%; TiO_2 is below detection limit. In the classification diagram of Hey (1954; not shown) all chlorites plot into the clinochlore field.

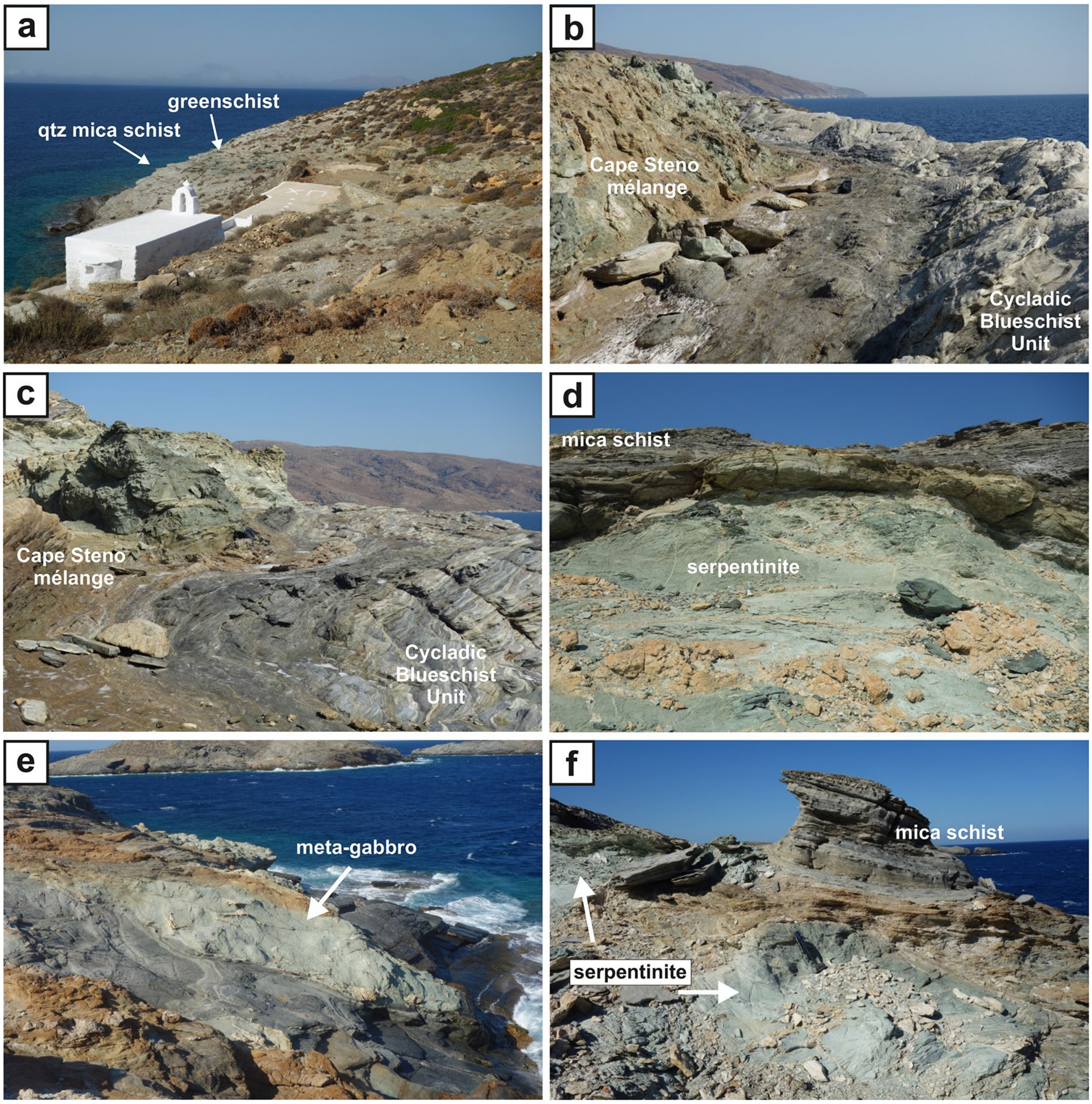

Fig. 2 Field images of the study areas in southern Andros (Cape Steno) and northern Tinos. **a** Outcrop of the Lower Unit at Agios Stefanos, Cape Steno. The U–Pb dated sample 8170 was collected in the basal siliciclastic sequence a few meters further back from the field of view. **b**, **c** Tectonic contact between the Lower Unit and the Cape Steno meta-ophiolites. **d** Serpentinite block overlain by mica schists in the Cape Steno mélange. **e** Meta-gabbro and **f** serpentinite blocks enclosed in schist sequences near Aghios Theodoros, Tinos

Cr-spinel and/or chromite record various stages of alteration into porous Fe-chromite, Cr-magnetite and magnetite (Online Resource 3, ESM Fig. 1). For the purpose of this study, only grains or domains that have retained their original composition are of interest. This includes Cr-spinel and/or chromite surrounded by porous Fe-chromite (type I) and chromite with magnetite rims of variable thickness (type II). Cr-spinels of the first group have Cr# [Cr# = Cr/(Cr + Al) atomic ratio] of 0.44–0.50, Mg# [Mg# = Mg/(Mg + Fe^{2+}) atomic ratio] of 0.62–0.40 (Fig. 3) and Fe^{3+}# [Fe^{3+}# = Fe^{3+}/(Fe^{3+} + Al + Cr) atomic ratio] of < 0.05. Chemical compositions are dominated by Cr_2O_3 (34.3–37.2 wt%), Al_2O_3 (30.4–25.3 wt%), FeO (14.2–19.2 wt%) and MgO (10.8–14.15 wt%). Fe_2O_3 concentrations range from 2.8 to 5.4 wt%. MnO and NiO concentrations are < 1.0 wt% and < 0.2 wt%, respectively. Type I chromites have a more variable chemical composition than Cr-spinels and are characterized by higher Cr# (0.50–0.80) and Fe^{3+}# (0.05–0.25) as well as lower Mg# (0.42 to < 0.10) (Fig. 3). Most chromites have Cr_2O_3 concentrations ranging from 31.2 to 42.7 wt% as well as variable Al_2O_3 and Fe_2O_3 contents (4.9–25.7 wt% and 4.2–18.3 wt%, respectively). Lower MgO (0.86–8.8 wt%) concentrations are balanced by higher FeO (21.7–30.1 wt%) and MnO (0.33–6.2 wt%) contents.

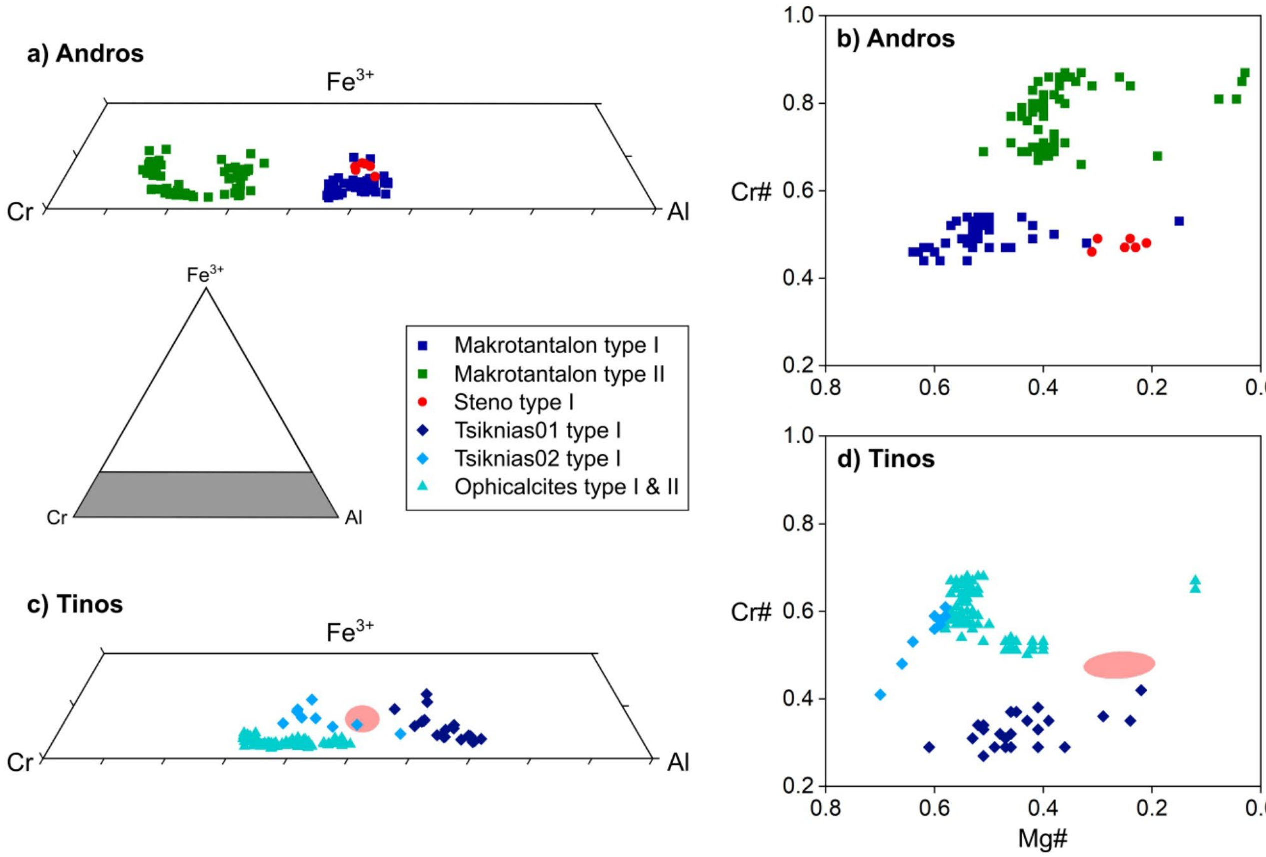

Fig. 3 Al^{3+}–Cr^{3+}–Fe^{3+} and Mg# vs. Cr# diagrams for chromian spinels with largely preserved original composition from Andros (**a**, **b**) and Tinos (**c**, **d**). Red-coloured fields in (**c**, **d**) indicate compositional field of the Cape Steno sample

NiO and TiO_2 contents vary between 0.05–0.16 wt% and 0.06–0.36 wt%, respectively. A second group of chromites (samples 8080, 8081, and 8083) is characterized by higher Cr_2O_3 (46.6–51.7 wt%) and low to moderate Al_2O_3 (3.0–13.3 wt%) and Fe_2O_3 (5.1–11.5 wt%) values.

Type II chromites have high Cr_2O_3 (48.5–59.6 wt%), low to moderate Al_2O_3 (5.8–16.4 wt%), and low Fe_2O_3 (2.1–6.3 wt%) concentrations. FeO ranges from 17.8 to 23.0 wt% and MgO varies between 5.8 and 10.5 wt%. Type II chromites have high Cr# (0.66–0.87), high to moderate Mg# (0.51–0.31) and low Fe^{3+}# (< 0.1). MnO concentrations (0.36–0.53 wt%) are lower than in type I spinels. NiO and TiO_2 contents are < 0.10 and < 0.20 wt%, respectively.

For samples from the MU on Andros, the Al_2O_3 vs. TiO_2 tectonic discrimination diagram (Fig. 4a) indicates the existence of two compositional groups. Type II Cr-spinels display SSZ affinity and plot in the high-Cr# area of the forearc field (Fig. 5b). Type I chromites have higher Al_2O_3 concentrations and lower Cr# values which are both compatible with a similar tectonic setting but overlap with the MORB peridotite field (Fig. 4). The type I chromites from Cape Steno show similar characteristics but with a stronger trend towards lower Mg# values, probably recording alteration (Fig. 4b). In samples from Tinos, two groups with different geotectonic affinities can be distinguished. Type I and II chromites of ophicalcites as well as some Tsiknias samples (Tsik02) have compositions in between the values of the Andros serpentinites, but samples from Tinos also include a distinct group of type I Cr-spinel (Tsik01) with a MORB affinity (Fig. 4).

White mica in the Cape Steno gneisses is phengite with Si values in the range from 3.27 to 3.65 but mostly display values > 3.5 (Fig. 5a-e). X_{Mg} [Mg/(Mg + Fe + Mn)] varies between 0.58 and 0.82 and X_{Na} [Na/(Na + K + Ca)] is < 0.1. Phengites of the jadeitite 5100 are characterized by Si-contents of 3.38–3.55. X_{Mg} is in the range from 0.42 to 0.68 and X_{Na} < 0.1. The white mica population of sample 8123 comprises phengites with Si-values of 3.38–3.5. X_{Mg} and X_{Na} values are 0.54–0.71 and < 0.1, respectively.

Clinopyroxene in sample 5100 comprises colourless and greenish grains (Online Resource 3, ESM Fig. 2) representing jadeite and omphacite (Fig. 5f).

Bulk rock geochemistry of serpentinites

A total of 61 serpentinite samples were selected for bulk rock geochemical studies. Analytical data is summarized

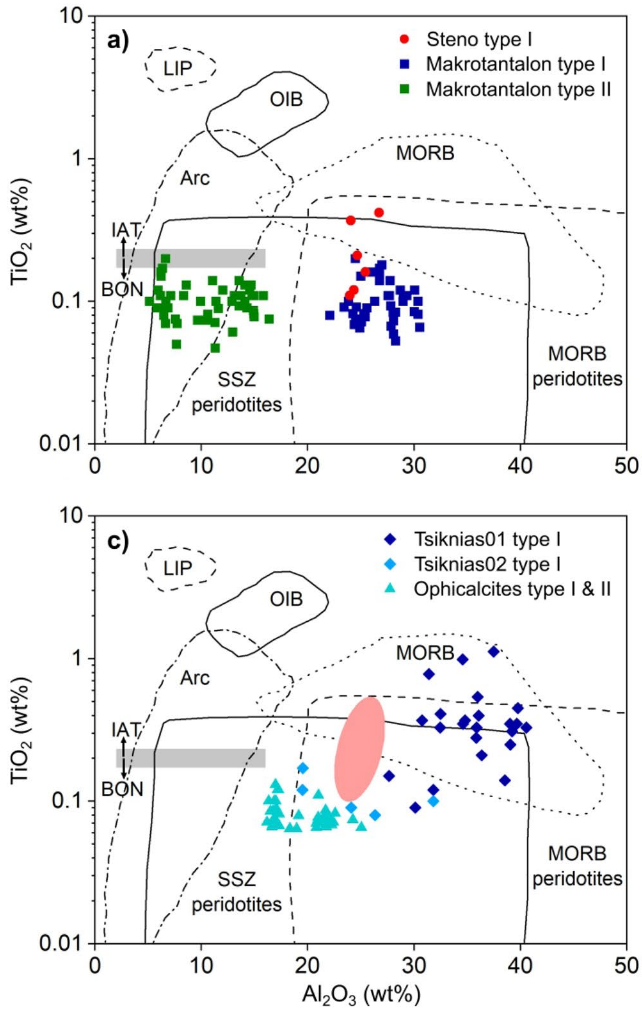

Fig. 4 Al_2O_3 vs. TiO_2 diagram (after Kamenetsky 2001) and Mg# vs. Cr# plot for chromian spinels from Andros (**a**, **b**) and Tinos (**c**, **d**). LIP = large igneous provinces; OIB = ocean island basalts; Arc = arc-related volcanic rocks (BON = boninites, IAT = island-arc-tholeiites); N-MORB = normal mid-ocean-ridge basalts; SSZ = supra-subduction zone mantle peridotites; MORB peridotites = MORB-like mantle peridotites. Fields in (**b**, **d**) from Kapsiotis (2014) and references therein

in Online Resource 5 and shown in Figs. 6 and 7. Data evaluation is based on a volatile-free basis. Major element compositions of serpentine-rich samples are dominated by high concentrations of SiO_2 (43.2–49.0 wt%; on an anhydrous basis) and MgO (31.8–47.9 wt%), and more variable FeO (5.4–16.5 wt%). Al_2O_3 contents are in the range of 0.2–4.7 wt%. CaO is mostly low (< 0.4 wt%) but especially in samples from Tinos higher contents were recognized (up to 4.1 wt%), due to the presence of secondary carbonates. MgO/SiO_2 and Al_2O_3/SiO_2 (anhydrous wt%) ratios are 0.65–1.09 and < 0.1, respectively. Mg# values (= molar $[Mg/(Mg + Fe^{2+})]$ vary between 0.77 and 0.93. Chlorite-rich samples contain considerably lower SiO_2 (31.4–37.4 wt%) and FeO (0.11–0.34 wt%) concentrations. MgO and CaO contents are 28.7–39.2 wt% and 0.18–1.68 wt%, respectively. MgO/SiO_2 and Al_2O_3/SiO_2 ratios are 0.88–1.05 and 0.19–0.62, respectively. Mg# values vary between 0.77 and 0.90. Both serpentine- and chlorite-dominated samples have mostly low TiO_2 and MnO contents (< 0.1–0.24 wt%), and moderate Cr_2O_3 (0.24–0.88 wt%) and NiO (0.10–0.47 wt%) concentrations. Loss on ignition (LOI) values of both rock varieties are in the 9.9–14.6 wt% range.

Cape Steno: most serpentinites display relatively flat, overall depleted CI-chondrite normalized REE patterns (Fig. 7). All samples show slight depletion from mid rare earth elements (MREE) to light rare earth elements (LREE) ($La_N/Sm_N = 0.89–0.46$) except sample 8115, which is characterized by a stronger enrichment of LREE compared to MREE ($La_N/Sm_N = 2.62$). REE patterns of samples 8118 and 8115 display Eu anomalies (Eu_N/Eu^*) of 1.39 and 0.76, respectively. Cape Steno samples are depleted compared to primitive mantle (PM) values and

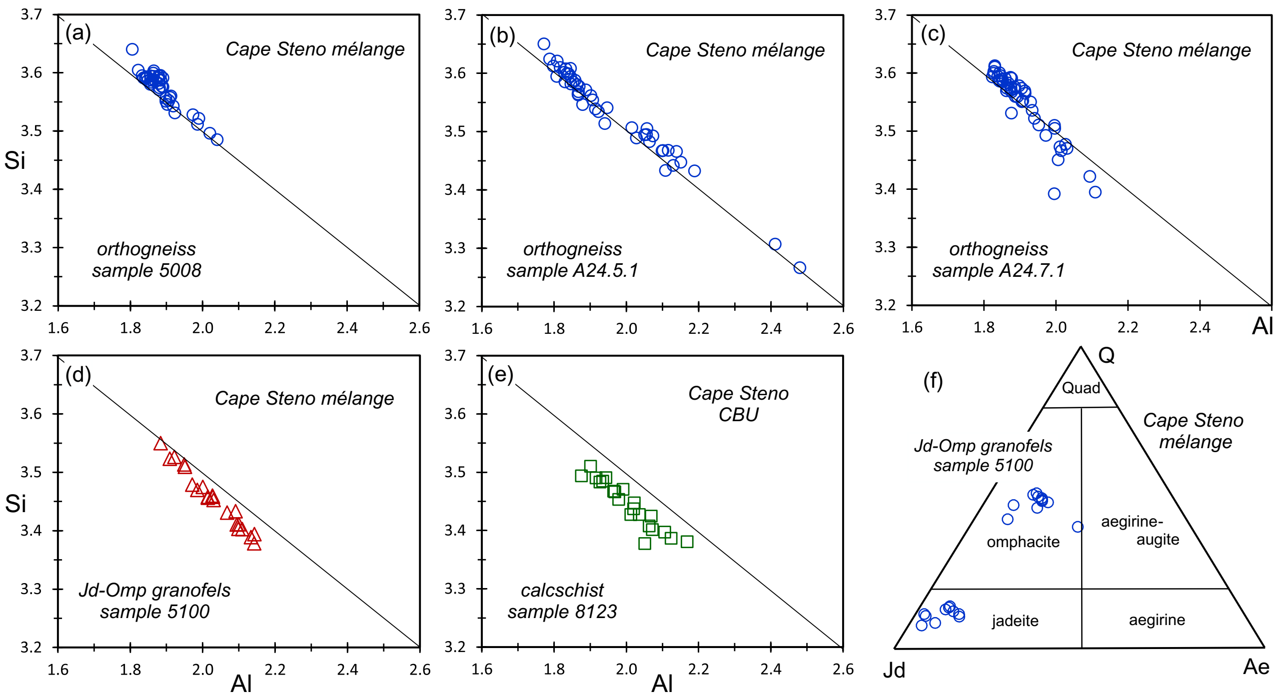

Fig. 5 **a** Si–Al diagram (atoms per formula unit) for white mica from the Cape Steno area. **b** Mineral composition of clinopyroxene in the classification diagram of Morimoto et al. (1988)

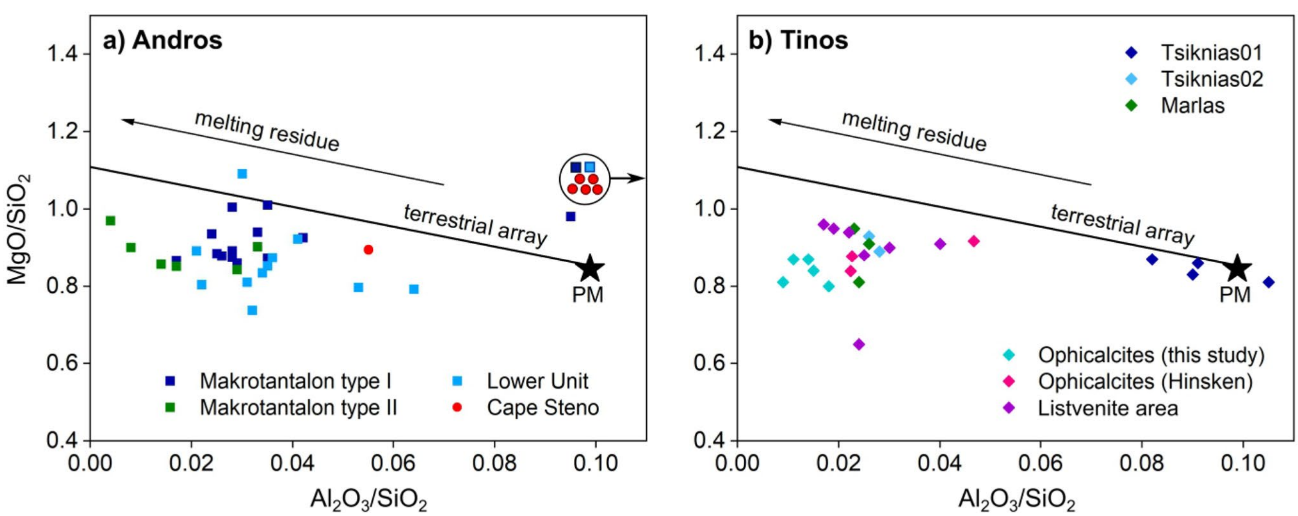

Fig. 6 Bulk rock Al_2O_3/SiO_2 vs. MgO/SiO_2 ratios of serpentinites from (**a**) Andros and (**b**) Tinos with data of this study and from Hinsken et al. (2017). Black line represents the "terrestrial array", indicating the trend from a primitive mantle to a harzburgitic composition (Jagoutz et al. 1979; Hart and Zindler 1986). PM value is from Sun and McDonough (1989). Data points in the circle plot are outside the displayed axis values

show distinct positive and negative peaks. Sample 8115 is characterized by enrichments in Cs, Th and U as well as depletion in Ta, Nb, Zr and Sr. The other Cape Steno ultramafic rocks show positive anomalies in Cs and Pb. Moreover, trace element patterns of samples 8116, 8117, and 8118 are marked by enrichments in high field strength elements (HFSE) and Sr. Samples 8119 and 8120 are depleted in Zr and Hf, but display peaks in U and Sr.

NW Andros: Most samples show weakly pronounced concave upward REE patterns with most samples displaying

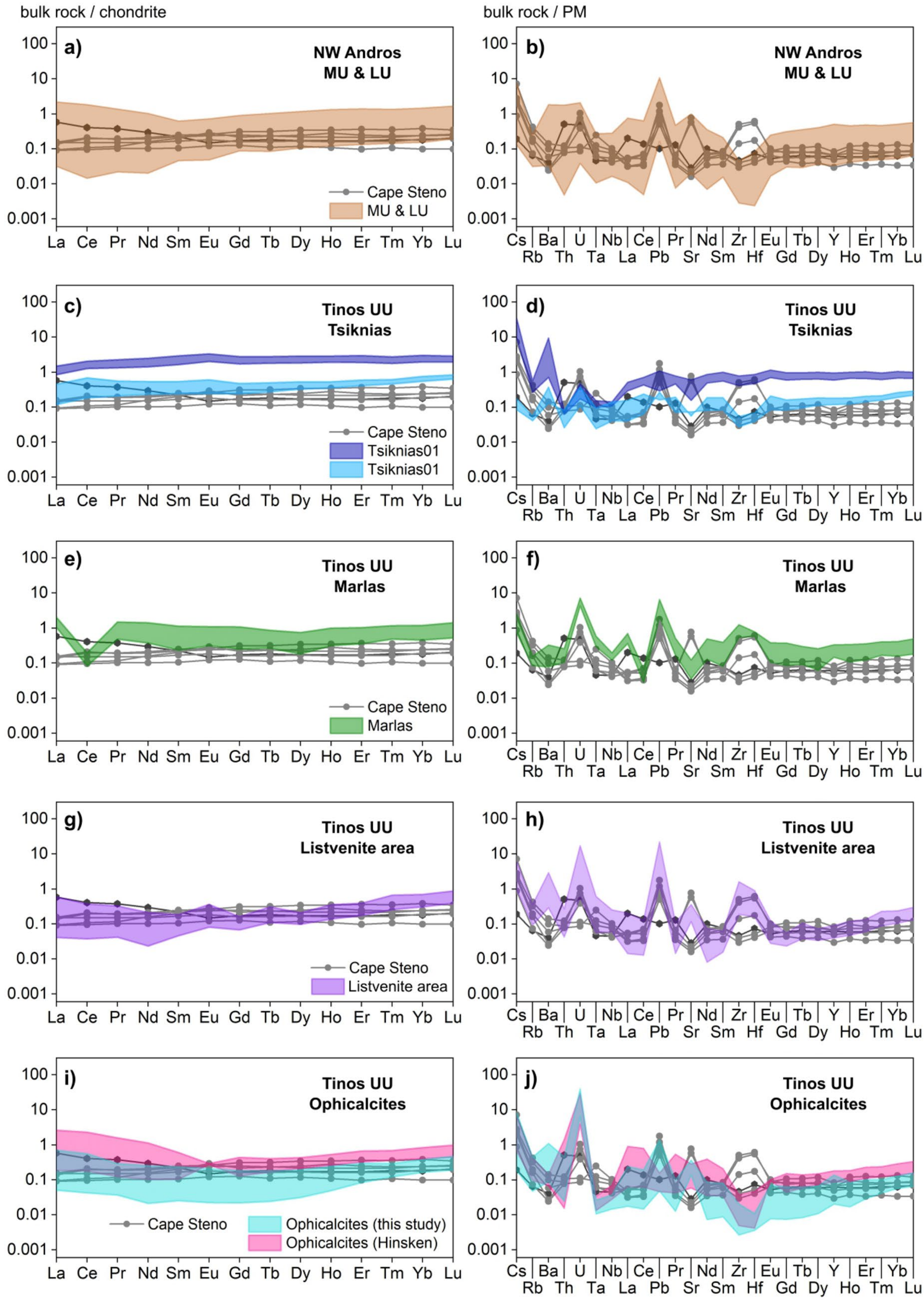

bulk rock / chondrite
bulk rock / PM
a)
NW Andros
MU & LU
Cape Steno
MU & LU
b)
NW Andros
MU & LU
c)
Tinos UU
Tsiknias
Cape Steno
Tsiknias01
Tsiknias01
d)
Tinos UU
Tsiknias
e)
Tinos UU
Marlas
Cape Steno
Marlas
f)
Tinos UU
Marlas
g)
Tinos UU
Listvenite area
Cape Steno
Listvenite area
h)
Tinos UU
Listvenite area
i)
Tinos UU
Ophicalcites
Cape Steno
Ophicalcites (this study)
Ophicalcites (Hinsken)
j)
Tinos UU
Ophicalcites
100
10
1
0.1
0.01
0.001
La Ce Pr Nd Sm Eu Gd Tb Dy Ho Er Tm Yb Lu
Cs Ba U Nb Ce Pr Nd Zr Eu Tb Y Er Yb
Rb Th Ta La Pb Sr Sm Hf Gd Dy Ho Tm Lu

◂**Fig. 7** Chondrite and primitive mantle (PM) normalized trace element compositions of Cape Steno serpentinites compared to similar rocks from NW Andros (without MU samples 8077 and 8091) and various occurrences of the Upper Unit on Tinos (Tsiknias, Marlas, listvenite and ophicalcite areas), including data of Hinsken et al. (2017) in (i) and (j). Normalizing values after Sun and McDonough (1989)

moderate to strong enrichment in LREE compared to MREE ($1.21 < La_N/Sm_N < 5.27$) as well as depletion in MREE compared to heavy rare earth elements (HREE) with Gd_N/Yb_N as low as 0.19 (Fig. 7a). However, samples 8095 and 8098 display a continuous enrichment from HREE to LREE, whereas samples 8089, 8096, and 8101 are characterized by a continuous depletion. There are no differences in the mineral assemblages of samples showing enrichments in LREE and those that are depleted in LREE compared to HREE. Trace element patterns of NW Andros samples have distinct peaks in fluid-mobile elements (FME) such as Cs, Ba, U and Pb. Sr can be enriched or depleted compared to neighboring elements. All PM normalized patterns show negative anomalies in Zr and Hf, often accompanied by depletion in other HFSE such as Ta and Nb.

Tinos: Trace element characteristics of serpentinites from different outcrop areas vary significantly. A subgroup of the Tsiknias samples (Tsik01) show flat HREE patterns with slight depletion towards LREE ($La_N/Sm_N = 0.63–0.45$) (Fig. 7c). REE compositions are almost chondritic, whereas the second group (Tsik02) shows a weak depletion from HREE to LREE ($Gd_N/Yb_N = 0.44$ and 0.62; $La_N/Sm_N = 0.49$ and 0.84, respectively). Both groups display small Eu anomalies ($Eu_N/Eu^* = 0.89–1.26$). PM normalized trace element patterns of Tsik01 samples indicate strong enrichments in Cs and Ba (Fig. 7d). HFSE and Sr are slightly to moderately depleted compared to neighboring elements. Tsik02 samples are depleted compared to PM values and display negative anomalies in HFSE as well as positive anomalies in Cs, Ba and U.

Ultramafic rocks from the Marlas area are characterized by weakly pronounced concave upward REE patterns with strong negative Ce anomalies ($Ce_N/Ce^* = 0.16–0.08$) (Fig. 7e). Trace element diagrams display moderate to strong enrichments in Cs, U, Pb, Zr and Hf as well as negative anomalies in Ce and Sr (Fig. 7f).

REE patterns of serpentinites from the listvenite area show strong depletions from HREE to MREE ($Gd_N/Yb_N = 0.14–0.37$) and positive Eu anomalies (1.39–2.87; Fig. 7g). Two samples are characterized by moderate to strong, negative Ce anomalies ($Ce_N/Ce^* = 0.29$ and 0.61). PM normalized trace element patterns display peaks for Cs, Ba, U, Pb, Sr as well as for the HFSE (Fig. 7h).

Samples from the ophicalcite occurrences have pronounced concave upward REE patterns with Ce (0.38–1.66) and Eu (0.74–1.41) anomalies (Fig. 7i). Samples 8140 and 8146 are less depleted in their REE compositions than the other samples. Concave upward patterns are also observed in PM normalized trace element diagrams (Fig. 7j). All samples show positive peaks in Cs, U, Pb and Sr as well as negative anomalies in HFSE.

Bulk rock composition of meta-gabbros

For comparison with similar rocks from Cape Steno, six meta-gabbro samples from the NW coast of Tinos (Agios Theodoros, Gavalas; Fig. 1c) were selected for bulk rock geochemistry. Analytical data is summarized in Online Resource 5 and shown in Fig. 8e–f. REE patterns are relatively flat with depletion towards LREE and small positive Eu anomalies. Trace element patterns normalized to PM values show depletions in HFSE (Zr, Hf, Nb, Th) but positive anomalies in Pb and Sr. Additionally, three samples show variable enrichments in Cs, Rb and Ba.

U–Pb and Rb–Sr geochronology

Zircon grains of sample 8170 have subhedral to variably rounded shapes (Fig. 9). CL imaging indicates a high number of grains with oscillatory zoning. Zircons with homogeneous or weak internal structures are also common. Some grains show patchy, banded, or sector-zoned CL patterns while a small number of zircons have low CL intensity. The filtered U–Pb data (181 out of 190 analyses) yielded an age range from 80 Ma to 2.7 Ga (Fig. 9; Online Resource 3, ESM Fig. 3; and Online Resource 6). The data show a broad maximum at 275–375 Ma with a peak at 315–360 Ma. Two small peaks show up at ca. 250 Ma ($n = 6$) and ca. 470 Ma ($n = 7$). A broad age cluster occurs at 500–700 Ma. Fifteen analyses yielded ages in the interval of 1.0–2.7 Ga. The youngest age occurs at ca. 80 Ma and is constrained by two grains with $^{238}U/^{206}Pb$ ages of 83 ± 2 Ma and 85 ± 3 Ma (2σ). Three zircons are characterized by Late Jurassic ages (147 ± 4 Ma, 164 ± 2 Ma, 165 ± 3 Ma). A well-constrained coherent age group occurs at ca. 290 Ma (Isoplot TuffZirc age: 294 + 6/–3 Ma, 98.4% confidence, $n = 7$; weighted average: 294 ± 3 Ma, MSWD = 0.53, probability = 0.78). The prominent Triassic age cluster recognized in detrital zircon populations of CBU samples in other parts of Andros, Tinos and Syros is here only represented by a small peak at ca. 250 Ma (Fig. 10). The age peaks at 315–360 Ma and 290–300 Ma are also common in siliciclastic rocks from the MU (Bröcker et al. 2016).

Rb–Sr analytical data and the isochron diagram of the calcschist sample 8123 are shown in Online Resource 3. Alignment of all datapoints representing sized fractions of phengite (5x), epidote (1x) and calcite (2x) indicate a Rb–Sr date of 28.5 ± 0.7 Ma (MSWD = 18). Exclusion of

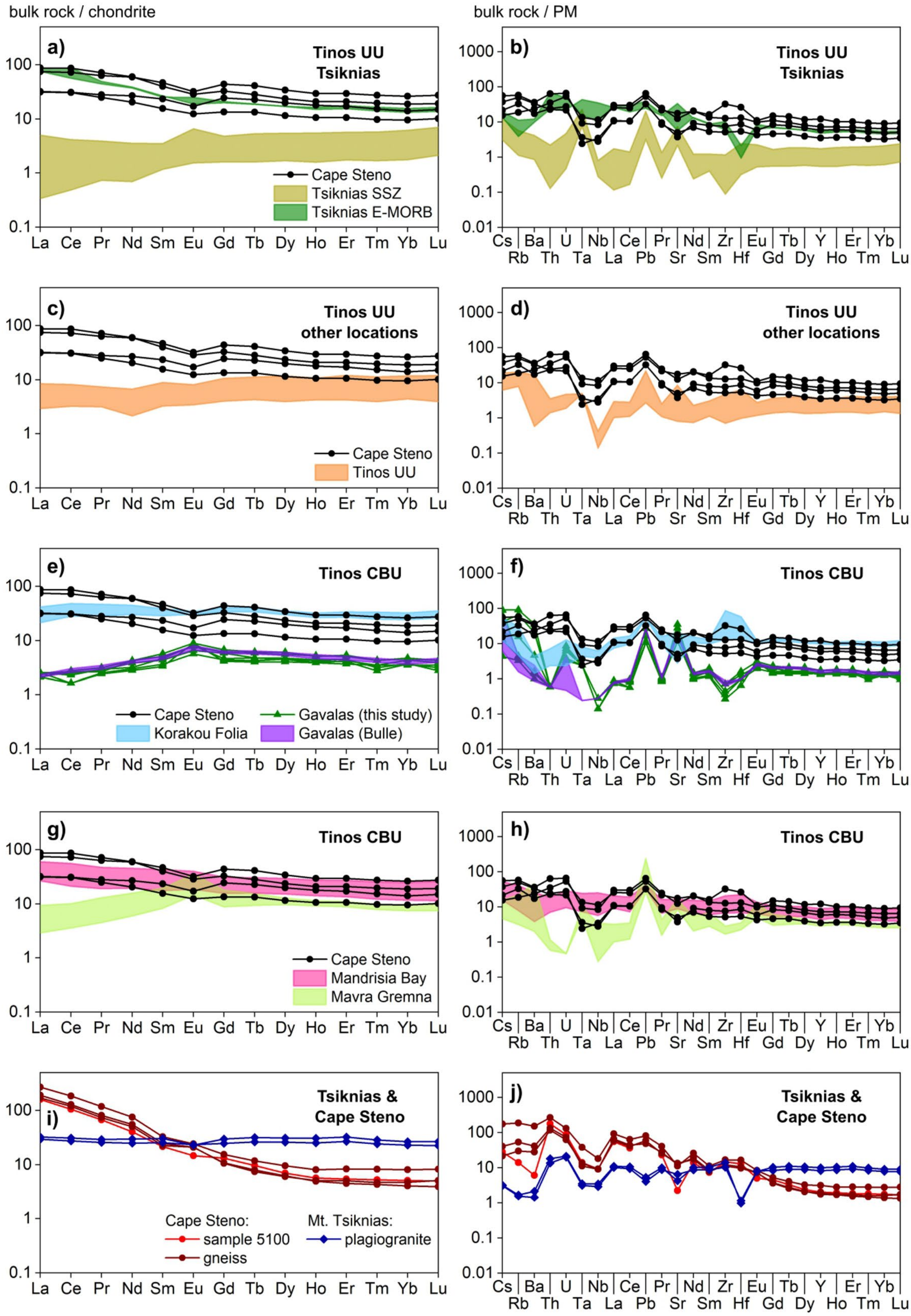
bulk rock / chondrite
bulk rock / PM
a)
Tinos UU
Tsiknias
Cape Steno
Tsiknias SSZ
Tsiknias E-MORB
b)
Tinos UU
Tsiknias
c)
Tinos UU
other locations
Cape Steno
Tinos UU
d)
Tinos UU
other locations
e)
Tinos CBU
Cape Steno
Gavalas (this study)
Korakou Folia
Gavalas (Bulle)
f)
Tinos CBU
g)
Tinos CBU
Cape Steno
Mandrisia Bay
Mavra Gremna
h)
Tinos CBU
i)
Tsiknias &
Cape Steno
Cape Steno:
sample 5100
gneiss
Mt. Tsiknias:
plagiogranite
j)
Tsiknias &
Cape Steno
0.1
1
10
100
1000
0.01
La Ce Pr Nd Sm Eu Gd Tb Dy Ho Er Tm Yb Lu
Cs Ba U Nb Ce Pr Nd Zr Eu Tb Y Er Yb
Rb Th Ta La Pb Sr Sm Hf Gd Dy Ho Tm Lu

◂**Fig. 8** Chondrite and primitive mantle (PM) normalized trace element compositions of Cape Steno meta-gabbros compared to similar rocks from the Upper Unit (**a**–**d**) and the CBU (**e**–**h**) from Tinos, and similar diagrams of Cape Steno gneisses and Tinos plagiogranites (**i**, **j**). Data are from Bulle et al. (2010), Bröcker et al. (2014), Lamont et al. (2020a), Mavrogonatos et al. (2021) and this study. Normalizing values after Sun and McDonough (1989)

the smallest mica grain size fraction from the straight-line fit results in a similar apparent age of 28.7 ± 0.5 Ma but a lower MSWD (6.7).

Discussion

The meta-ophiolitic rocks occurring in block-in-matrix sequences of the study area yielded Jurassic (Andros) and Late Cretaceous (Tinos) U–Pb zircon ages (Bröcker and Pidgeon 2007; Bulle et al. 2010). This age difference either indicates the existence of a single mélange containing rock fragments with different protolith ages, or the existence of two mélanges belonging to distinct tectonic subunits. Recently reported Jurassic protolith ages of meta-ophiolitic rocks from the Tsiknias Ophiolite on Tinos (Lamont et al. 2020a) imply that the Cape Steno mélange may represent a previously misinterpreted occurrence of the UCU. A correlative relationship to the undated serpentinite belt stretching across NW Andros (Fig. 1b) cannot be ruled out yet either, especially as the geological map of Papanikolaou (1978a, b) indicates that both occurrences have a similar structural position above the uppermost marble horizon (m4) of the LU.

Are there supportive arguments for a correlation between the Cape Steno rock suite and the serpentinites of NW Andros or Tinos?

A discontinuous belt of mappable serpentinite bodies (up to several hundred meter in size) extends through NW Andros (Papanikolaou 1978a, b). Huyskens and Bröcker (2014) described this belt as a suitable marker of the tectonic contact between the MU and LU but avoided a clear allocation of the ultramafic rocks to one of the two nappes. Based on lithostratigraphic observations, Papanikolaou (1978b) interpreted the ultramafic rocks as an olistostromatic horizon in the upper parts of the LU, placing the tectonic contact above the serpentinite belt. In contrast, Shin (2014) suggested that the serpentinites belong to the MU, inferring a tectonic contact at some distance below the ultramafic rocks. Based on new mapping, Gerogiannis et al. (2019) concluded that the serpentinite bodies are exposed at different structural levels within both tectonic units and thus cannot be used for delineating the nappe contact. Gerogiannis et al. (2019) used lithological contrasts between both nappes and the presence of mylonitic rocks for demarcation of the MU-LU boundary. In contrast to Cape Steno, serpentinites of NW Andros are not found together with other meta-ophiolitic rocks in the same outcrop, but a meta-gabbro block with well-preserved igneous texture and relics of sodic amphibole was described from nearby schists of the MU (Huyskens and Bröcker 2014).

Using the geological map of Gerogiannis et al. (2019) as reference, we have systematically studied ultramafic rocks collected on both sides of the inferred tectonic contact. However, systematic differences in the chromian spinel or bulk rock geochemistry that correlate with the tectonic assignment were not recognized. Rather, these rocks represent a largely homogeneous sample suite, whose original composition has been modified by alteration processes. Bulk rock Al_2O_3/SiO_2 and MgO/SiO_2 ratios plot at the refractory end of the "terrestrial array" (Jagoutz et al. 1979; Hart and Zindler 1986) indicating that these samples were derived from ultramafic precursors which had experienced moderate to high degrees of partial melting (Fig. 6). The low Al_2O_3 contents suggest harzburgitic protoliths. There are no bulk rock compositional features that would allow discriminating between serpentinites of the MU and LU. This observation also applies to the mineral chemistry of chromian spinel. Most samples ascribed to the MU have primary Cr-spinel/chromite compositions suggesting supra-subduction zone and forearc affinities (Fig. 4a, b). We tentatively interpret the existence of distinct compositional groups of Cr-spinel/chromite as an expression of different degrees of partial melting. In samples assigned to the LU, the original chromite and/or chromian spinels were completely erased by superimposed alteration. The serpentinites of NW Andros either belong to different tectonic units but have identical geochemical compositions or occur within the same tectonic unit. Since the serpentinites are mainly exposed in the vicinity of the tectonic contact, their distribution could indicate the existence of a wider fault zone, possibly due to folding of the tectonic contact zone during exhumation (Gerogiannis et al. 2019).

The ultramafic rocks from NW Andros show little or no compositional similarities with the serpentinites from Cape Steno which lack HFSE depletions and show overall flatter REE patterns than serpentinites from the northern part of the island (Fig. 7a, b). Geochemical characteristics of ultramafic rocks do not provide clear indications for a correlative relationship between the meta-ophiolites of NW and SE Andros, but this could result from a stronger metasomatic overprint of the Cape Steno serpentinites. With the exception of sample 8115, bulk rock Al_2O_3/SiO_2 and MgO/SiO_2 ratios of Cape Steno ultramafic rocks deviate considerably from the melting trend, indicating severe alteration that is expressed by almost complete chloritization. It should also be noted that ultramafic rocks from the Upper Unit of Tinos show differences in the mineral and bulk rock geochemistry between different outcrop areas which, however, all belong to the same tectonic unit

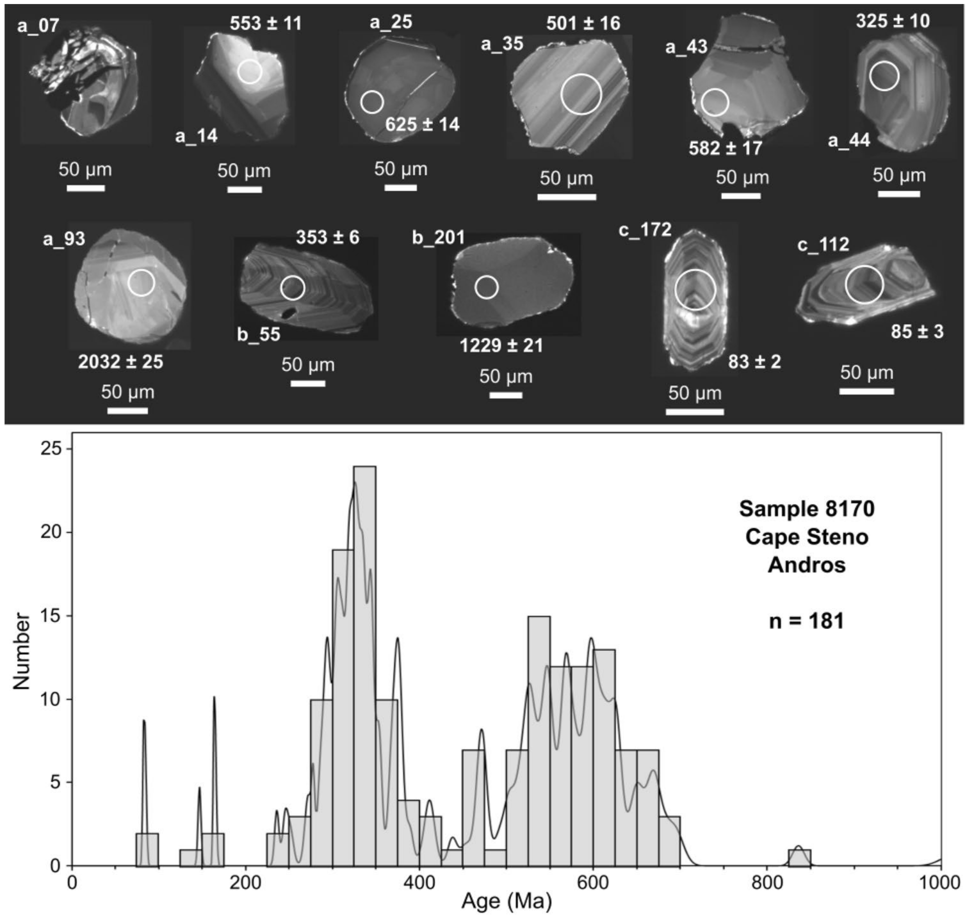

Fig. 9 **a** Selected CL images of detrital zircons from sample 8170 (Cape Steno, S Andros). White circles indicate LA-ICP-MS spots, corresponding ages are given in Ma. **b** Probability distribution diagram with histogram of sample 8170 from Cape Steno (S Andros) showing zircon data < 1000 Ma. Bin width = 25 Ma

(Fig. 7c–j). Likewise, the meta-gabbro blocks in the LU on Tinos represent a geochemically heterogenous group (Fig. 8 e–h) within the same tectonic unit.

In the absence of clear superimposed alteration trends (Fig. 6), the compositional differences among the Tinos serpentinites are interpreted as primary characteristics, possibly related to different degrees of partial melting. MgO/SiO_2 and Al_2O_3/SiO_2 ratios and PM like trace element compositions document a more primitive character of the Tsik01 samples than for the other serpentinites from this island (Figs. 6, 7). REE and trace element characteristics of the Cape Steno serpentinites are in good agreement with some of the Tsiknias samples (Tsik02), and with samples from the Marlas and listvenite areas (Fig. 7c–f). A possible co-genetic relationship to the meta-ophiolitic rocks of the Tsiknias area is further indicated by whole rock geochemical similarities of meta-gabbros from both occurrences (Fig. 8a, b), and their corresponding Jurassic protolith ages (Bröcker and Pidgeon 2007; Lamont et al 2020a). However, unambiguous evidence of a HP/LT metamorphic history leaves no doubt that the Cape Steno mélange is not part of the UU.

Evidence of a high-pressure metamorphic overprint of the Cap Steno rock suite

Andros and Tinos are only separated by a narrow sea channel (ca. 1500 m) and on both islands the metamorphic succession comprises marbles, schists and meta-ophiolitic block-in-matrix sequences (Buzaglo-Yoresh et al. 1995; Bulle et al. 2010; Bröcker et al. 2016). The Cape Steno mélange was originally interpreted as a meta-olistostrome (Mukhin 1996), and considered to represent the topmost part of the LU (Papanikolaou 1978a, b; Buzaglo-Yoresh 1995; Bröcker and Pidgeon 2007; Bulle et al. 2010), suggesting a HP/LT metamorphic history. This interpretation is based on (1) field relationships and petrographic similarities with the metamorphic succession of NW Tinos where various meta-igneous blocks, partly with HP/LT mineral assemblages, occur in meta-sedimentary host rocks with a clear blueschist-facies record, and (2) the presence of jadeitite in the Cape Steno block assemblage leading to the assumption that formation conditions correspond to those of similar rocks in the HP/LT serpentinite mélange on Syros (Buzaglo-Yoresh 1995; Bulle et al. 2010). Other explanations include the possibility that the Cape Steno rock suite represents a tectonic unit with a different metamorphic record than the

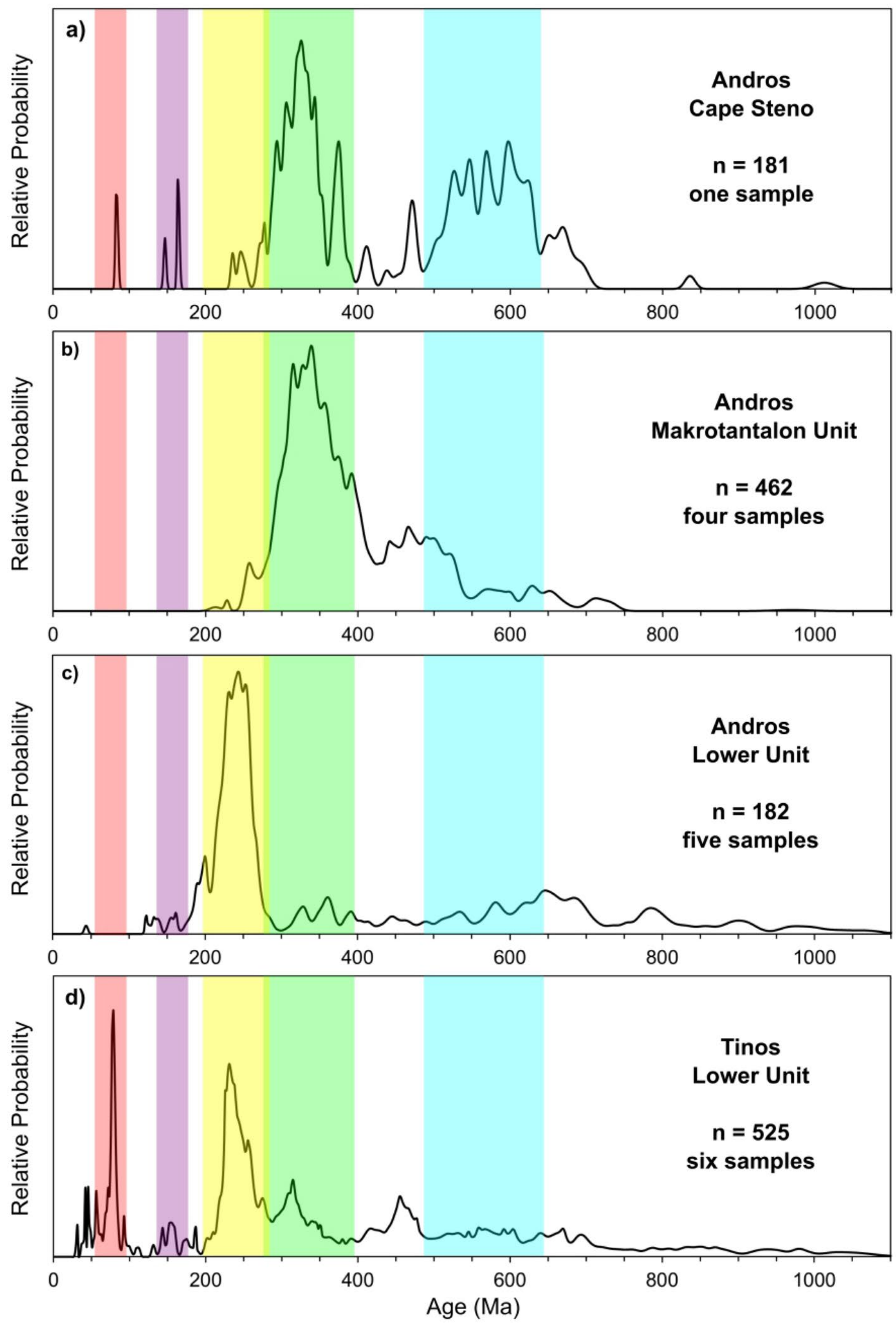

Fig. 10 Probability distribution diagrams of detrital zircon from **a** Cape Steno (this study), **b** Makrotantalon Unit, **c** Lower Unit of Andros (Bröcker et al. 2016) and **d** Lower Unit of Tinos (Bulle et al. 2010; Hinsken et al. 2016)

CBU, that tectonic or sedimentary processes caused mixing of CBU rocks with fragments of other origin, or that the Cape Steno jadeitite was formed at different *P*–*T* conditions.

A relationship of jadeitite to ancient subduction complexes is clearly established (e.g. Harlow et al. 2015 and references therein) but formation of this rock type is not limited to peak blueschist- or eclogite-facies conditions. Temporal discrepancies between jadeitite formation and peak HP metamorphism recorded in other blocks of the same mélange were described from several occurrences (Tsujimori and Harlow 2012), indicating that jadeitite can already form in the overlying mantle wedge at T = 200–400 °C and P = 0.6–1.2 GPa (Tsujimori and Harlow 2012; Harlow et al. 2015). Jadeitite formation was also described from epidote amphibolite-facies *P*–*T* regimes (Tsujimori and Harlow 2012; Harlow et al. 2015).

At this point, the petrogenesis of the Cape Steno jadeitite remains unclear, but this rock type clearly differs from the jadeitites of the Cycladic HP/LT mélanges in terms of bulk-rock composition, age complexity of the zircon population and protolith age. The jadeitites of the CBU are characterized by homogeneous zircon populations which only yielded a single Late Cretaceous U–Pb age group (Bröcker and Enders 1999, 2001; Bulle et al. 2010). In contrast, the Cape Steno jadeitite is characterized by a more complex zircon population with Jurassic overgrowths (163.1 ± 3.9 Ma and 174.3 ± 2.0 Ma) on Middle Proterozoic (ca. 1126 Ma and ca. 1421 Ma) and Permian (ca. 273 Ma and ca. 281 Ma) grains (Bulle et al. 2010). The Jurassic ages of the overgrowths broadly correspond to the protolith ages of meta-gabbros and meta-plagiogranitic gneisses (156.2 ± 2.3 Ma, 160.0 ± 2.0 Ma) from the same occurrence (Bröcker and Pidgeon 2007). Furthermore, the REE and trace element patterns of jadeitites from the CBU and Andros are different (Bröcker and Enders 1999, 2001; Bulle et al. 2010). In the case of Andros, the REE patterns of both jadeitite and cpx-free gneisses are characterized by a strong enrichment in LREE ($La_N/Yb_N = 29–44$), whereas jadeitites and omphacitites from Tinos and Syros often show sinusoidal REE variations, concave REE patterns, weak LREE enrichment ($La_N/Yb_N = 1.6–2.2$) or a continuously increasing REE distribution from La to Lu (Online Resource 3, ESM Fig. 4; Bröcker and Enders 2001; Bulle et al. 2010). We therefore consider it unlikely that the Cape Steno jadeitite represents an exotic fragment of the CBU but instead assume a different origin and *P–T* history.

In meta-gabbros and felsic gneisses, relics of blue amphibole were not recognized but high-Si values of phengitic mica in the gneisses (3.5–3.6 per formula unit; Fig. 5; Online Resource 4) clearly document that these rocks were affected by HP/LT metamorphism. The lack of HP/LT assemblages in the meta-gabbros is not at variance to a high-pressure history. Similar observations were also reported from some meta-gabbros of the CBU on Tinos (Bulle et al. 2010). Besides bulk rock compositional differences, short duration of metamorphism, lack of deformation, and limited availability of fluids or infiltration paths may explain the lack of equilibrium mineral assemblages.

Is the Cape Steno mélange a previously misinterpreted outcrop of the Makrotantalon Unit?

Field observations, geochemical and geochronological data can be reconciled by two scenarios: (1) Two distinct mélanges are exposed in SE Andros and NW Tinos that belong to different tectonic units with different tectono-metamorphic histories, both containing HP/LT rocks related to the same or different metamorphic events. The Cape Steno rock suite is correlative with the MU of NW Andros and is separated by a tectonic contact from the meta-olistostromatic sequences of the LU. The mélange exposed near Aghios Theodoros, NW Tinos, could be a lateral equivalent of the Cape Steno mélange. (2) The Cape Steno mélange is a litho- or tectonostratigraphic equivalent of the metamorphic succession exposed in NW Tinos which can be clearly assigned to the LU. The different jadeitites were formed almost simultaneously from precursor rocks with different protolith ages. In this case, the existence of Jurassic meta-igneous blocks in mélanges of the CBU would be documented for the first time.

We consider the first alternative as the more likely explanation and suggest a correlative relationship of the Cape Steno mélange with the Makrotantalon Unit of NW Andros. The MU records a more complex polymetamorphic history than other tectonic subunits of the CBU, including Early Cretaceous and Eocene blueschist-facies events (Huyskens and Bröcker 2014; Huet et al. 2015; Gerogiannis et al. 2019). Unequivocal evidence of Cretaceous HP/LT metamorphism in the CBU has not yet been documented (for a discussion of contrasting views see Fu et al. 2010, 2012; Bulle et al. 2010), but occurs in the Pelagonian zone of mainland Greece (e.g. Schermer et al. 1990; Lips et al. 1998). Accordingly, Huet et al. (2015) suggested a Pelagonian affinity for the MU. The coexistence of both Cretaceous and Eocene HP/LT rocks led to the interpretation that the MU was incorporated into the nappe stack of the CBU at deep subduction levels during the Eocene or somewhat earlier, resulting in a common metamorphic history since that time (Gerogiannis et al. 2019). New Rb–Sr dates of blueschist-facies rocks of the MU (Bröcker et al., unpublished data) further substantiate interpretations suggesting that the MU was affected by both Cretaceous and Eocene blueschist-facies events.

The combination of Pelagonian meta-ophiolitic rocks and HP/LT metamorphism suggests a correlative relationship between the Cape Steno rock suite and the MU which both occur in a similar litho- or tectonostratigraphic position overlying the topmost part of the LU (Papanikolaou 1978a, b). Jurassic protolith ages are unknown from the HP/LT mélanges of the CBU. So far, all dated meta-ophiolitic rock fragments only yielded Late Cretaceous U–Pb zircon ages (Keay 1998; Tomaschek et al. 2003; Bulle et al. 2010; Bröcker and Keasling 2006; Bröcker et al. 2014). Furthermore, Triassic protolith ages (249–240 Ma) were reported for gneisses of the Syros mélange (Bröcker and Keasling 2006) and felsic meta-igneous rocks from Andros considered to represent either olistoliths of a meta-olistostrome or fragments related to large-scale boudinage (Bröcker and Pidgeon 2007).

Is it justified to correlate the schists below the Cape Steno mélange with similar rock sequences in NW Tinos?

Lithological characteristics and similarities in the tectono-metamorphic history indicate that the marble-schist sequences of SE Andros and NW Tinos represent lateral equivalents. In NW Tinos, meta-ophiolitic blocks (meta-gabbros, glaucophanites, serpentinites) are more widespread than in southern Andros but generally are rather rare constituents in siliciclastic host rocks (Buzaglo-Yoresh 1995; Bulle et al. 2010). Mineral assemblages of the LU on both islands mostly indicate greenschist-facies conditions, but mineralogical evidence of earlier HP/LT metamorphism was not completely erased. Relics of sodic amphiboles are often found.

Similar maximum depositional ages of ca. 80 Ma provide further evidence of a correlative relationship between schist sequences on both islands (Bulle et al. 2010; Shin 2014; this study). Such ages are a typical feature of detrital zircon populations of the CBU on Tinos and Syros (Bulle et al. 2010; Löwen et al. 2015; Hinsken et al. 2016) and were also recognized in the newly studied sample 8170, collected directly below the Cape Steno mélange, interpreted to represent the topmost part of the CBU in SE Andros.

The Rb–Sr date of a calcschist (28.7 ± 0.5 Ma; Online Resource 3; ESM Fig. 4) from Cape Steno, collected close to the tectonic contact at Aghios Stephanos, corresponds to similar Rb–Sr dates (~ 29–25 Ma) from other parts of Andros and Tinos (Huyskens and Bröcker 2014), lending support to the assumption that this date could indicate a distinct *P*–*T*–*D* stage during exhumation affecting both islands.

Summary and conclusions

This study focused at unravelling the status of the Cape Steno mélange within the structural architecture of the Cyclades. The Cape Steno occurrence is different to the HP/LT mélanges of the CBU on the neighboring islands of Syros and Tinos (e.g. Dixon and Ridley 1987; Bröcker and Enders 2001; Bröcker and Keasling 2006; Bulle et al. 2010; Gyomlai et al. 2021). The combination of Jurassic meta-ophiolites and HP/LT metamorphism is unusual and a unique feature. Judging from field observations, geochronological and bulk rock geochemical data, we consider a relationship to the Makrotantalon Unit of NW Andros to be very likely. The MU represents a distinct tectonic subunit of Pelagonian derivation in the nappe stack of the CBU that is mainly exposed in NW Andros, but possibly correlates with the Ochi nappe on Evia (Papanikolaou, 2013; Gerogiannis et al. 2019). The MU includes serpentinites and rare meta-gabbro in a marble-schist sequence that was affected by both Cretaceous and Eocene HP/LT episodes (e.g. Huet et al. 2015; Gerogiannis et al. 2019). The meta-gabbros and serpentinites exposed on the NW coast of Tinos could also represent remnants of this Pelagonian nappe, but so far there is insufficient evidence to support this assumption. Lithological and mineralogical criteria, maximum depositional ages and similarities in the tectono-metamorphic evolution suggest that the schist sequence below the Cape Steno mélange corresponds to the CBU on Tinos which was only affected by Eocene HP/LT metamorphism.

Supplementary Information The online version contains supplementary material available at https://doi.org/10.1007/s00531-022-02161-w.

Acknowledgements This work was supported by a grant of the Deutsche Forschungsgemeinschaft (BR 1068/26-1). We thank Beate Schmitte for her help with the LA-ICP-MS and Heidi Baier for supporting Rb–Sr analyses.

Funding Open Access funding enabled and organized by Projekt DEAL. Deutsche Forschungsgemeinschaft (BR 1068/26–1).

Declarations

Conflict of interest None.

Availability of data and material Full dataset available as Online Resource.

Code availability Not applicable.

Open Access This article is licensed under a Creative Commons Attribution 4.0 International License, which permits use, sharing, adaptation, distribution and reproduction in any medium or format, as long as you give appropriate credit to the original author(s) and the source, provide a link to the Creative Commons licence, and indicate if changes were made. The images or other third party material in this article are included in the article's Creative Commons licence, unless indicated otherwise in a credit line to the material. If material is not included in the article's Creative Commons licence and your intended use is not permitted by statutory regulation or exceeds the permitted use, you will need to obtain permission directly from the copyright holder. To view a copy of this licence, visit http://creativecommons.org/licenses/by/4.0/.

References

Avigad D, Garfunkel Z (1989) Low angle shear zones underneath and above a blueschist belt - Tinos Island, Cyclades, Greece. Terra Nova 1:182–187. https://doi.org/10.1111/j.1365-3121.1989.tb00350.x

Brichau S, Ring U, Carter A, Monié P, Bolhar R, Stockli D, Brunel M (2007) Extensional faulting on Tinos Island, Aegean Sea, Greece: How many detachments? Tectonics. https://doi.org/10.1029/2006TC001969

Bröcker M, Enders M (1999) U-Pb zircon geochronology of unusual eclogite-facies rocks from Syros and Tinos (Cyclades, Greece). Geol Mag 136:111–118. https://doi.org/10.1017/S0016756899002320

Bröcker M, Enders M (2001) Unusual bulk-rock compositions in eclogite-facies rocks from Syros and Tinos (Cyclades, Greece): implications for U-Pb zircon geochronology. Chem Geol 175:581–603. https://doi.org/10.1016/S0009-2541(00)00369-7

Bröcker M, Franz L (1998) Rb–Sr isotope studies on Tinos Island (Cyclades, Greece): Additional time constraints for metamorphism, extent of infiltration-controlled overprinting and deformational activity. Geol Mag 135:369–382. https://doi.org/10.1017/S0016756898008681

Bröcker M, Franz L (2005) The base of the Cycladic blueschist unit on Tinos Island (Greece) re-visited: Field relationships, phengite chemistry and Rb–Sr geochronology. N Jahrb Mineral Abh 181:81–93. https://doi.org/10.1127/0077-7757/2005/0181-0003

Bröcker M, Franz L (2006) Dating metamorphism and tectonic juxtaposition on Andros Island (Cyclades, Greece): Results of a Rb–Sr study. Geol Mag 143:609–620. https://doi.org/10.1017/S0016756806002 41X

Bröcker M, Keasling A (2006) Ionprobe U-Pb zircon ages from the high-pressure/low-temperature mélange of Syros, Greece: age diversity and the importance of pre-Eocene subduction. J Metamorph Geol 24:615–631. https://doi.org/10.1111/j.1525-1314.2006.00658.x

Bröcker M, Pidgeon RT (2007) Protolith ages of meta-igneous and meta-tuffaceous rocks from the Cycladic blueschist unit, Greece: Results of a reconnaissance U-Pb zircon study. J Geol 115:83–98. https://doi.org/10.1086/509269

Bröcker M, Kreuzer H, Matthews A, Okrusch M (1993) $^{40}Ar/^{39}Ar$ and oxygen isotope studies of polymetamorphism from Tinos Island, Cycladic blueschist belt. J Metamorph Geol 11:223–240. https://doi.org/10.1111/j.1525-1314.1993.tb00144.x

Bröcker M, Bieling D, Hacker B, Gans P (2004) High-Si phengite records the time of greenschist-facies overprinting: Implications for models suggesting mega-detachments in the Aegean Sea. J Metamorph Geol 22:427–442. https://doi.org/10.1111/j.1525-1314.2004.00524.x

Bröcker M, Baldwin S, Arkudas R (2013) The geologic significance of $^{40}Ar/^{39}Ar$ and Rb–Sr white mica ages from Syros and Sifnos, Greece: a record of continuous (re)crystallization during exhumation? J Metamorph Geol 31:629–646. https://doi.org/10.1111/jmg.12037

Bröcker M, Löwen K, Rodionov N (2014) Unraveling protolith ages of meta-gabbros from Samos and the Attic-Cycladic Crystalline Belt, Greece: results of a U-Pb zircon and Sr–Nd whole rock study. Lithos 198–199:234–248. https://doi.org/10.1016/j.lithos.2014.03.029

Bröcker M, Huyskens M, Berndt J (2016) U-Pb dating of detrital zircons from Andros, Greece: constraints for the time of sediment accumulation in the northern part of the Cycladic blueschist belt. Geol J 51:354–367. https://doi.org/10.1002/gj.2634

Bulle F, Bröcker M, Gärtner C, Keasling A (2010) Geochemistry and geochronology of HP mélanges from Tinos and Andros, Cycladic blueschist belt, Greece. Lithos 117:61–81. https://doi.org/10.1016/j.lithos.2010.02.004

Buzaglo-Yoresh A, Matthews A, Garfunkel Z (1995) Metamorphic evolution on Andros and Tinos – a comparative study. In: Arkin Y, Avigad D (Eds.), Israel Geological Society Annual Meeting 1995, p16

Buzaglo-Yoresh A (1995) Petrology and metamorphic history of southern Andros and northern Tinos (Cyclades). Master Thesis, Hebrew University Jerusalem

Cliff RA, Bond CE, Butler RWH, Dixon JE (2017) Geochronological challenges posed by continuously developing tectonometamorphic systems, insights from Rb–Sr mica ages from the Cycladic Blueschist Belt, Syros (Greece). J Metamorphic Geol 35:197–211

Cooperdock EHG, Raia NH, Barnes JD, Stockli DF, Schwarzenbach EM (2018) Tectonic origin of serpentinites on Syros, Greece: Geochemical signatures of abyssal origin preserved in a HP/LT subduction complex. Lithos 296–299:352–364. https://doi.org/10.1016/j.lithos.2017.10.020

Deschamps F, Godard M, Guillot S, Hattori KH (2013) Geochemistry of subduction zone serpentinites: a review. Lithos 178:96–127. https://doi.org/10.1016/j.lithos.2013.05.019

Dixon JE, Ridley J (1987) Syros. In: Helgeson HC (ed) Chemical transport in metasomatic processes. Reidel Publishing Company, Dordrecht, pp 489–501

Dürr S (1986) Das Attisch-kykladische Kristallin. In: Jacobshagen V (ed) Geologie von Griechenland. Gebrüder Bornträger, Berlin, pp 116–148

Dürr S, Altherr R, Keller J, Okrusch M, Seidel E (1978) The Median Aegean Crystalline Belt: stratigraphy, structure, metamorphism, magmatism. In: Closs H, Roeder DH, Schmidt K (eds) Alps, Appeninnes, Hellenides. Schweizerbart, Stuttgart, pp 455–477

Flansburg ME, Stockli DF, Poulaki EM, Soukis K (2019) Tectono-magmatic and stratigraphic evolution of the Cycladic basement, Ios Island. Greece Tectonics 38(7):2291–2316. https://doi.org/10.1029/2018TC005436

Forster MA, Lister GS (2005) Several distinct tectono-metamorphic slices in the Cycladic eclogite–blueschist belt, Greece. Contrib Mineral Petrol 150:523–545. https://doi.org/10.1007/s00410-005-0032-9

Fu B, Valley JW, Kita NT, Spicuzza MJ, Paton C, Tsujimori T, Bröcker M, Harlow GE (2010) Multiple origins of zircons in jadeitite. Contrib Mineral Petrol 159:769–780. https://doi.org/10.1007/s00410-009-0453-y

Fu B, Paul B, Cliff J, Bröcker M, Bulle F (2012) O-Hf isotope constraints on the origin of zircon in high-pressure mélange blocks and associated matrix rocks from Tinos and Syros, Greece. Eur J Mineral 24:277–287. https://doi.org/10.1127/0935-1221/2011/0023-2131

Fu B, Bröcker M, Ireland T, Holden P, Kinsley LPJ (2015) Zircon U-Pb, O, and Hf isotopic constraints on Mesozoic magmatism in the Cyclades, Aegean Sea, Greece. Int J Earth Sci 104:75–87. https://doi.org/10.1007/s00531-014-1064-z

Gerogiannis N, Xypolias P, Chatzaras V, Aravadinou E, Papapavlou K (2019) Deformation within the Cycladic subduction-exhumation channel: new insights from the enigmatic Makrotantalo nappe (Andros, Aegean). Int J Earth Sci 108:817–843. https://doi.org/10.1007/s00531-019-01680-3

Glodny J, Ring U (2021) The Cycladic Blueschist Unit of the Hellenic subduction orogen: Protracted high-pressure metamorphism, decompression and reimbrication of a diachronous nappe stack. Earth Sci Rev. https://doi.org/10.1016/j.earscirev.2021.103883

Gyomlai Z, Agard P, Marschall HR, Jolivet L, Gerdes A (2021) Metasomatism and deformation of block-in-matrix structures in Syros: The role of inheritance and fluid-rock interactions along the subduction interface. Lithos 386–387:105996

Harlow GE, Tsujimori T, Sorensen SS (2015) Jadeitites and plate tectonics. Annu Rev Earth Planet Sci 43:105–138. https://doi.org/10.1146/annurev-earth-060614-105215

Hart SR, Zindler A (1986) In search of a bulk-Earth composition. Chem Geol 57:247–267

Hey MH (1954) A new review of the chlorites. Mineral Mag 30:277–292. https://doi.org/10.1180/minmag.1954.030.224.01

Hinsken T, Bröcker M, Berndt J, Gärtner C (2016) Maximum sedimentation ages and provenance of metasedimentary rocks from Tinos Island, Cycladic blueschist belt, Greece. Int J Earth Sci 105:1923–1940. https://doi.org/10.1007/s00531-015-1258-z

Hinsken T, Bröcker M, Strauss H, Bulle F (2017) Geochemical, isotopic and geochronological characterization of listvenite from the Upper Unit on Tinos, Cyclades, Greece. Lithos 282–283:281–297. https://doi.org/10.1016/j.lithos.2017.02.019

Huet B, Labrousse L, Monié P, Malvoisin B, Jolivet L (2015) Coupled phengite ^{40}Ar–^{39}Ar geochronology and thermobarometry: P-T-t evolution of Andros Island (Cyclades, Greece). Geol Magn 152:711–727. https://doi.org/10.1017/S0016756814000661

Huyskens M, Bröcker M (2014) The status of the Makrotantalon Unit (Andros, Greece) within the structural framework of the Attic-Cycladic Crystalline Belt. Geol Mag 151:430–446. https://doi.org/10.1017/S0016756813000307

Jagoutz E, Palme H, Baddenhausen H, Blum K, Cendales M, Dreibus G, Spettel B, Wänke H, Lorenz V (1979) The abundances of

major, minor and trace elements in the earth's mantle as derived from primitive ultramafic nodules. Proc Lunar Planet Sci Conf 10th 2:2031–2050.
Kamenetsky VS (2001) Factors Controlling Chemistry of Magmatic Spinel: an empirical study of associated olivine, Cr-spinel and melt inclusions from primitive rocks. J Petrol 42:655–671. https://doi.org/10.1093/petrology/42.4.655
Kapsiotis A (2014) Composition and alteration of Cr-spinels from Milia and Pefki serpentinized mantle peridotites (Pindos Ophiolite Complex, Greece). Geol Carp 65(1):83–89. https://doi.org/10.2478/geoca-2013-0006
Katzir Y, Matthews A, Garfunkel Z, Schliestedt M (1996) The tectono-metamorphic evolution of a dismembered ophiolite (Tinos, Cyclades, Greece). Geol Mag 133:237–254. https://doi.org/10.1017/S0016756800008992
Keay S (1998) The Geological Evolution of the Cyclades, Greece: Constraints from SHRIMP U–Pb Geochronology. Dissertation, Australian National University, Canberra. https://doi.org/10.25911/5d66671ad2b2f
Lagos M, Scherer EE, Tomaschek F, Münker C, Keiter M, Berndt J, Ballhaus C (2007) High precision Lu–Hf geochronology of Eocene eclogite-facies rocks from Syros, Cyclades, Greece. Chem Geol 243:16–35
Lamont TN, Roberts NMW, Searle MP, Gopon P, Waters DJ, Millar I (2020a) The Age, Origin, and Emplacement of the Tsiknias Ophiolite, Tinos, Greece. Tectonics 39, e2019TC005677. http://doi.org/https://doi.org/10.1029/2019TC005677
Lamont TN, Searle MP, Gopon P, Roberts NMW, Wade J, Palin RM, Waters DJ (2020b) The Cycladic Blueschist Unit on Tinos, Greece: Cold NE subduction and SW directed extrusion of the Cycladic continental margin under the Tsiknias Ophiolite. Tectonics 39, e2019TC005890. https://doi.org/10.1029/2019TC005890
Laurent V, Jolivet L, Roche V, Augier R, Scaillet S, Cardello GL (2016) Strain localization in a fossilized subduction channel: Insights from the Cycladic Blueschist Unit (Syros, Greece). Tectonophysics 672:150–169. https://doi.org/10.1016/j.tecto.2016.01.036
Laurent V, Huet B, Labrousse L, Jolivet L, Monie P, Augier R (2017) Extraneous argon in high-pressure metamorphic rocks: Distribution, origin and transport in the Cycladic Blueschist Unit (Greece). Lithos 272:315–335
Lips A, White SH, Wijbrans JR (1998) $^{40}Ar/^{39}Ar$ laserprobe direct dating of discrete deformational events: a continuous record of early Alpine tectonics in the Pelagonian Zone, NW Aegean area, Greece. Tectonophysics 298:133–153. https://doi.org/10.1016/S0040-1951(98)00181-4
Löwen K, Bröcker M, Berndt J (2015) Depositional ages of clastic metasediments from Samos and Syros, Greece: results of a detrital zircon study. Int J Earth Sci 104:205–220. https://doi.org/10.1007/s00531-014-1058-x
Martha SO, Dörr W, Gerdes A, Petschick R, Schastok J, Xypolias P, Zulauf G (2016) New structural and U-Pb zircon data from Anafi crystalline basement (Cyclades, Greece): constraints on the evolution of a Late Cretaceous magmatic arc in the Internal Hellenides. Int J Earth Sci 105:2031–2060. https://doi.org/10.1007/s00531-016-1346-8
Mavrogonatos C, Magganas A, Kati M, Bröcker M, Voudouris P (2021) Ophicalcites from the Upper Tectonic Unit on Tinos, Cyclades, Greece: mineralogical, geochemical and isotope evidence for their origin and evolution. Int J Earth Sci 110:809–832. https://doi.org/10.1007/s00531-021-01991-4
Mehl C, Jolivet L, Lacombe O, Labrousse L, Rimmele G (2007) Structural evolution of Andros (Cyclades, Greece): a key to the behaviour of a (flat) detachment within an extending continental crust. In The geodynamics of the Aegean and Anatolia (eds T Taymaz, Y Yilmaz and Y Dilek), pp. 41–73. Geological Society of London, Special Publication no. 291. http://doi.org/https://doi.org/10.1144/SP291.3
Melidonis NG (1980) The geological structure and mineral deposits of Tinos island (Cyclades, Greece). Geol Greece 13:1–80
Mukhin P (1996) The metamorphosed olistostromes and turbidites of Andros Island, Greece, and their tectonic significance. Geol Mag 133:697–711. https://doi.org/10.1017/S0016756800024559
Okrusch M, Bröcker M (1990) Eclogite facies rocks in the Cycladic blueschist belt, Greece: a review. Eur J Mineral 2:451–478. https://doi.org/10.1127/ejm/2/4/0451
Papanikolaou D (1978b) Contribution to the geology of the Aegean Sea; the island of Andros. Ann Géol Pays Hellén 29:477–553
Papanikolaou D (1987) Tectonic Evolution of the Cycladic Blueschist Belt (Aegean Sea, Greece). In: Helgeson HC (ed) Chemical Transport in Metasomatic Processes. Reidel Publishing Company, Dordrecht, pp 429–450
Papanikolaou D (2013) Tectonostratigraphic models of the Alpine terranes and subduction history of the Hellenides. Tectonophysics 595–596:1–24
Papanikolaou D (1978a) Geologic map of Greece. Andros Island, 1:50.000. Institute of Geological and Mining Research (IGME), Athens
Parra T, Vidal O, Jolivet L (2002) Relation between the intensity of deformation and retrogression in blueschist metapelites of Tinos Island (Greece) evidenced by chlorite-mica local equilibria. Lithos 63:41–66. https://doi.org/10.1016/S0024-4937(02)00115-9
Patzak M, Okrusch M, Kreuzer H (1994) The Akrotiri unit on the island of Tinos, Cyclades, Greece: Witness to a lost terrane of Late Cretaceous age. Neues Jahrb Geol Paläontol Abh 194:211–252
Peillod A, Ring U, Glodny J, Skelton A (2017) An Eocene/Oligocene blueschist/greenschist-facies *P-T* loop from the Cycladic Blueschist Unit on Naxos Island, Greece: Deformation-related reequilibration vs thermal relaxation: J Metamorphic Geol 35:805–830. https://doi.org/10.1111/jmg.12256
Philippon M, Brun JP, Gueydan F (2012) Deciphering subduction from exhumation in the segmented Cycladic Blueschist Unit (Central Aegean, Greece). Tectonophysics 524:116–134
Ring U, Laws S, Bernet M (1999) Structural analysis of a complex nappe sequence and late-orogenic basins from the Aegean Island of Samos, Greece. J Struct Geol 21:1575–1601
Ring U, Layer PW, Reischmann T (2001) Miocene high-pressure metamorphism in the Cyclades and Crete, Aegean Sea, Greece: Evidence for large-magnitude displacement on the Cretan detachment. Geology 29:395–398
Ring U, Glodny J, Will J, Thomson SN (2010) The Hellenic subduction system: high-pressure metamorphism, exhumation, normal faulting, and large-scale extension. Annu Rev Earth Planet Sci 38:45–76. https://doi.org/10.1146/annurev.earth.050708.170910
Robertson AHF (2002) Overview of the genesis and emplacement of Mesozoic ophiolites in the Eastern Mediterranean. Lithos 65:1–67. https://doi.org/10.1016/S0024-4937(02)00160-3
Schermer ER, Lux DR, Burchfiel BC (1990) Temperature-time history of subducted continental-crust, Mount Olympos Region. Greece Tectonics 9(5):1165–1195. https://doi.org/10.1029/TC009i005p01165
Shaked Y, Avigad D, Garfunkel Z (2000) Alpine high-ressure metamorphism of the Almyropotamos window (southern Evia, Greece). Geol Mag 137:367–380
Shin TA (2014) Tectonic evolution of Aegean metamorphic core complexes, Andros and Tinos Island, Greece. Master thesis, University of Texas at Austin, https://repositories.lib.utexas.edu/handle/2152/26449
Sun SS, McDonough WF (1989) Chemical and isotopic systematics of oceanic basalts: Implications for mantle composition and processes. In: Saunders AD, Norry MJ (eds) Magmatism in the ocean basins Geological Society, London, Special Publications 42:313–345. https://doi.org/10.1144/GSL.SP.1989.042.01.19
Tomaschek F, Kennedy AK, Villa IM, Lagos M, Ballhaus C (2003) Zircons from Syros, Cyclades, Greece - recrystallization and

mobilization of zircon during high-pressure metamorphism. J Petrol 44:1977–2002. https://doi.org/10.1093/petrology/egg067

Tsujimori T, Harlow GE (2012) Petrogenetic relationships between jadeitite and associated high-pressure and low-temperature metamorphic rocks in worldwide jadeitite localities: a review. Eur J Mineral 24:371–390. https://doi.org/10.1127/0935-1221/2012/0024-2193

Wijbrans JR, Schliestedt M, York D (1990) Single grain argon laser probe dating of phengites from the blueschist to greenschist transition on Sifnos (Cyclades, Greece). Contrib Mineral Petrol 104:582–593

Zeffren S, Avigad D, Heimann A, Gvirtzman Z (2005) Age resetting of hanging wall rocks above a low-angle detachment shear zone: Tinos Island (Aegean Sea). Tectonophysics 400:1–25. https://doi.org/10.1016/j.tecto.2005.01.003